USAARL Report No. 96-06

Evaluation of an Energy Absorbing Truck Seat for Increased Protection from Landmine Blasts

By

Nabih M. Alem
and
Gregory D. Strawn

Aircrew Protection Division
U.S. Army Aeromedical Research Laboratory
Fort Rucker, Alabama

Prepared for

Countermine Division
Night Vision & Electronic Sensors Directorate
Fort Belvoir, Virginia

19960227 109

January 1996

Approved for public release; distribution unlimited.

U.S. Army Aeromedical Research Laboratory
Fort Rucker, Alabama 36362-0577

Notice

Qualified requesters

Qualified requesters may obtain copies from the Defense Technical Information Center (DTIC), Cameron Station, Alexandria, Virginia 22314. Orders will be expedited if placed through the librarian or other person designated to request documents from DTIC.

Change of address

Organizations receiving reports from the U.S. Army Aeromedical Research Laboratory on automatic mailing lists should confirm correct address when corresponding about laboratory reports.

Disposition

Destroy this document when it is no longer needed. Do not return it to the originator.

Disclaimer

The views, opinions, and/or findings contained in this report are those of the author(s) and should not be construed as an official Department of the Army position, policy, or decision, unless so designated by other official documentation. Citation of trade names in this report does not constitute an official Department of the Army endorsement or approval of the use of such commercial items.

Reviewed:

KEVIN T. MASON
LTC(P), MC, MFS
Director, Aircrew Protection
Division

ROGER W. WILEY, O.D., Ph.D.
Chairman, Scientific
Review Committee

Released for publication:

DENNIS F. SHANAHAN
Colonel, MC, MFS
Commanding

Unclassified
SECURITY CLASSIFICATION OF THIS PAGE

REPORT DOCUMENTATION PAGE

Form Approved
OMB No. 0704-0188

1a. REPORT SECURITY CLASSIFICATION
Unclassified

1b. RESTRICTIVE MARKINGS

2a. SECURITY CLASSIFICATION AUTHORITY

3. DISTRIBUTION / AVAILABILITY OF REPORT
Approved for public release, distribution unlimited

2b. DECLASSIFICATION / DOWNGRADING SCHEDULE

4. PERFORMING ORGANIZATION REPORT NUMBER(S)
USAARL Report No. 96-06

5. MONITORING ORGANIZATION REPORT NUMBER(S)

6a. NAME OF PERFORMING ORGANIZATION
U.S. Army Aeromedical Research Laboratory

6b. OFFICE SYMBOL (If applicable)
MCMR-UAD

7a. NAME OF MONITORING ORGANIZATION
U.S. Army Medical Research and Materiel Command

6c. ADDRESS (City, State, and ZIP Code)
P.O. Box 620577
Fort Rucker, AL 36362-0577

7b. ADDRESS (City, State, and ZIP Code)
Fort Detrick
Frederick, MD 21702-5012

8a. NAME OF FUNDING / SPONSORING ORGANIZATION
Night Vision and Electronic Sensors Directorate

8b. OFFICE SYMBOL (If applicable)
STRBE-JES

9. PROCUREMENT INSTRUMENT IDENTIFICATION NUMBER

8c. ADDRESS (City, State, and ZIP Code)
10101 Gridley Road, Suite 104
Fort Belvoir, VA 22060-5818

10. SOURCE OF FUNDING NUMBERS

PROGRAM ELEMENT NO.	PROJECT NO.	TASK NO.	WORK UNIT ACCESSION NO.

11. TITLE (Include Security Classification)
Evaluation of an energy-absorbing truck seat for increased protection from landmine blasts

12. PERSONAL AUTHOR(S)
Nabih M. Alem and Gregory D. Strawn

13a. TYPE OF REPORT	13b. TIME COVERED FROM / TO	14. DATE OF REPORT (Year, Month, Day)	15. PAGE COUNT
Final			

16. SUPPLEMENTAL NOTATION

17. COSATI CODES			18. SUBJECT TERMS (Continue on reverse if necessary and identify by block number)
FIELD	GROUP	SUB-GROUP	mine blast, energy-absorbing, manikins, truck seat, tolerance threshold

19. ABSTRACT (Continue on reverse if necessary and identify by block number)

Mine blast resistant kits, developed by the Night Vision and Electronic Sensors Directorate (NVESD), are designed to enhance the survivability of the crew of military 5-ton trucks. The kit includes an energy-absorbing (EA) seat which is the focus of this report. A full-scale demonstration mine blast of a 5-ton truck was conducted using the full protection kit and included two anthropomorphic manikins to represent the passenger and driver. Only the passenger manikin was seated in the EA seat, while the driver manikin was seated in a standard seat. This report presents the analysis of test data performed by the U.S. Army Aeromedical Research Laboratory (USAARL). Results show the standard seat produced lumbar (lower back) spine compression of 2159 lbs, a value that exceeds the 1500-lb threshold generally used in spinal injury assessment. On the other hand, the EA prototype seat limited the compression of the lower spine to about 1329 lbs, a value which is below injury thresholds. The report concludes that NVESD mine protection kit reduced upward truck accelerations transmitted to the truck occupants and eliminated head contact injuries, and the EA seat reduced lumbar spine compressive forces by 38 percent to a level below tolerance threshold.

20. DISTRIBUTION / AVAILABILITY OF ABSTRACT
☒ UNCLASSIFIED/UNLIMITED ☐ SAME AS RPT. ☐ DTIC USERS

21. ABSTRACT SECURITY CLASSIFICATION
Unclassified

22a. NAME OF RESPONSIBLE INDIVIDUAL	22b. TELEPHONE (Include Area Code)	22c. OFFICE SYMBOL
Chief, Science Support Center	(334) 255-6907	MCMR-UAX-SI

DD Form 1473, JUN 86 *Previous editions are obsolete.*

SECURITY CLASSIFICATION OF THIS PAGE
Unclassified

SUPPLEMENTARY

INFORMATION

ERRATA - AD-A304297

United States Army Aeromedical Research Laboratory,
Fort Rucker, Alabama 36362-0577

USAARL Report No. 96-06 "Evaluation of an Energy Absorbing Truck Seat for Increased Protection from Landmine Blasts" by

Nabih M. Alem
and
Gregory D. Strawn

Aircrew Protection Division
U.S. Army Aeromedical Research Laboratory
Fort Rucker, Alabama
January 1996

Please replace page 13/14 in the subject report with the attached page 13/14 (References/Figure 1).

DTIC QUALITY INSPECTED 4

References

Air Standardization Coordinating Committee. 1989. Six-degree-of-freedom evaluation method. ASCC advisory publication 61/66, 10 May 1989.

Department of Defense. 1981. General specification for seats, helicopter cabin, crashworthy. Washington, DC: Department of Defense. MIL-S-85510(AS). 19 November.

Department of Defense. 1993. General specification for seat system, upward ejection, aircraft. Washington, DC: Department of Defense. MIL-S-9479C(USAF). 20 October.

Desjardins, S. P., Zimmermann, R. E., Bolukbasi, O., and Merritt, N. A. 1989. Aircraft crash survival design guide. Fort Eustis, VA: U.S. Army Aviation Research and Technology Activity. USAAVSCOM TR 89-D-22D.

Federal Aviation Regulation. 1993. Airworthiness standards: transport category rotorcraft, Part 29. §29.562, Emergency landing dynamic crashworthiness, section (c)(7). Washington, DC: Federal Aviation Administration.

Haley, J. L., Jr., and Palmer, R. W. 1995. Evaluation of a retrofit OH-58 pilot's seat to prevent back injury. Fort Rucker, AL: U.S. Army Aeromedical Research Laboratory, USAARL Report No. 95-9.

Mertz, H. J. 1984. Injury assessment values used to evaluate Hybrid III response measurements. Washington, DC: National Highway Transportation Safety Administration. NHTSA Docket 74-14, Notice 32, Enclosure 2 Of Attachment I of Part III of General Motions Submission USG 2284. March 22.

Mertz, H. J. 1993. Anthropomorphic Test Devices. *Accidental injury: Biomechanics and prevention,* chapter 4. Alan Nahum, John Melvin (editors). New York: Springer-Verlag.

National Highway Traffic Safety Administration. 1993. Federal Motor Vehicle Safety Standard. FMVSS20849 CFR Ch. V (10-1-93 Edition), §571.208, S6.1.2 and S6.1.3.

Ripple, G. R., and Mundie, T. G., ed. 1989. Medical evaluation of nonfragment injury effects in armored vehicle live fire tests - instrumentation requirements and injury criteria. Washington, DC: Walter Reed Army Institute of Research. Report AD-A233-058. September 1989.

Society of Automotive Engineers. Instrumentation for impact tests - SAE recommended practice. Warrendale, PA: Society of Automotive Engineers. SAE J211 Jun80.

Replacement page

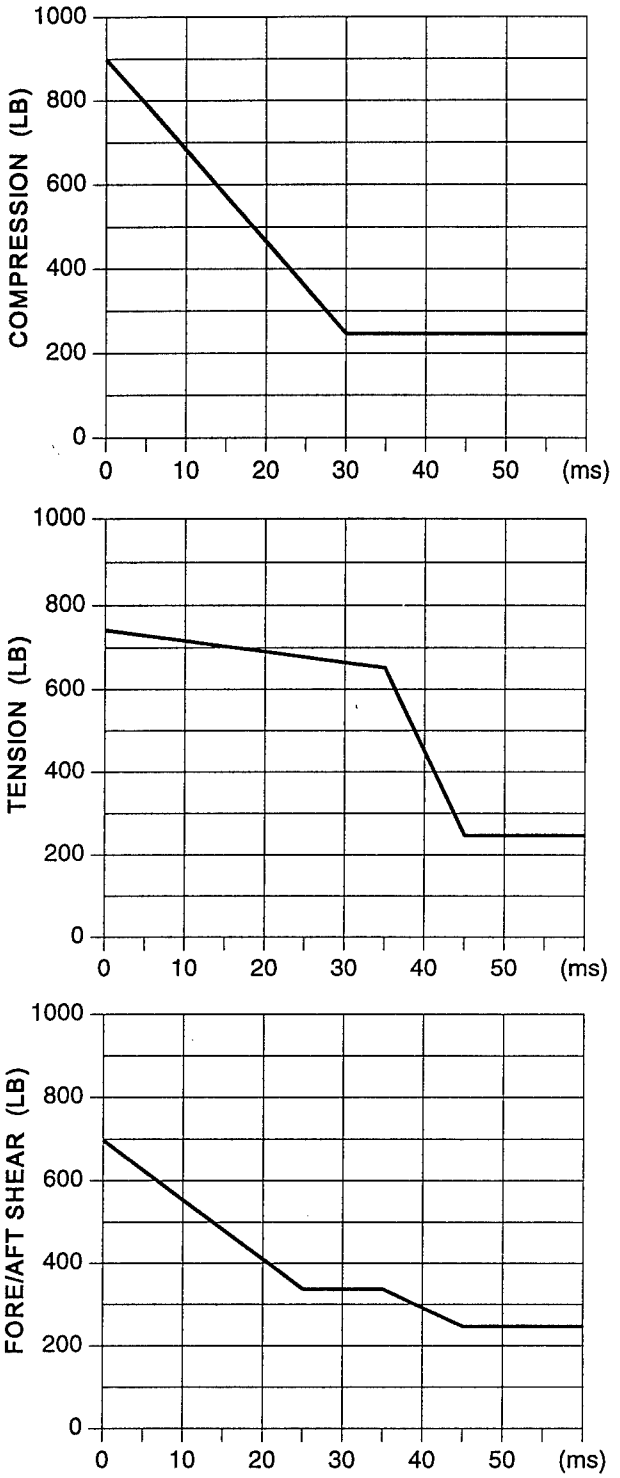

Figure 1. Injury assessment criteria curves for neck forces in compression, tension and shear loads.

Replacement page

Table of contents

List of figures

List of tables

Introduction

The Night Vision and Electronic Sensors Directorate (NVESD) has been engaged in a research and development effort to design, test, and deliver land mine resistant kits that protect the driver and passenger of M925A1 5-ton military trucks from land mine explosions. As part of this effort, an energy-absorbing (EA) seat was designed under a contract with Simula, Inc. to reduce the blast forces transmitted to the seated crew through the cabin floor and seat structure.

To evaluate the new EA design, a demonstration test was conducted on 8 December 1994 (test 120895) where the full protection kit that included the new EA seat was installed on a test truck and exposed to the blast of a mine placed centrally under the truck. In this test, two anthropomorphic manikins, i.e., crash dummies normally used in automotive testing, were used as surrogates of the driver and passenger. The passenger seat was replaced by the EA seat, while the driver seat was left unmodified.

Test data were provided to Simula, Inc., the designer of the seat, and to JAYCOR, another contractor performing risk assessment of blast effects. The same data also were given to the U.S. Army Aeromedical Research Laboratory (USAARL), Fort Rucker, Alabama, who is providing NVESD with additional consultation in design goals, test methodology, and risk assessment of acceleration effects. The test data included accelerations taken at the truck bumper, cabin floor, and new passenger seat, accelerations at the centers of mass of head, chest, and pelvis of each manikin, and forces at the lumbar (lower back) and the cervical (neck) areas of the spine.

This report presents the results of USAARL's data analysis of test no. 120894.

Objectives

1. Assess the injury risks to the head, neck, chest, and lumbar spine of the passenger when seated in the newly designed Simula seat, and compare to injury risks to the driver seated in the unmodified truck seat.

2. Determine the improvement in crew protection due to energy-absorbing seat design by comparing the responses of the two manikins.

3. Determine the effects of filtering on impact severity, and examine the response of articulated rigid body crash simulators to extremely short duration pulses.

4. Evaluate instrumentation methods used in the test and recommend alternate methods to improve the quality of the data in future mine blast tests.

Methods

Zero adjustment

Most instrumentation hardware leave a zero imbalance, sometimes referred to as a DC bias, in the signals which must be removed for accurate analysis. A 100-msec preimpact quiescent period was provided in the 120894 test data for this purpose, but was not used. Instead, a flat postimpact segment, typically between 500 to 800 ms, was designated to be the true "zero" state which should be removed. This resulted in a nonzero preimpact state for the transducers. Because the 100-msec preimpact segment does not contribute to the impact dynamics, it was reasonably set to zero to provide an important perspective on the initiation of impact.

Signal filtering

The analysis is dictated by the type of data available from the test. Since the data are in the form of digital signals, mostly from the crash dummies, the Society of Automotive Engineers (SAE) J211 guidelines were applied. SAE J211 guideline (SAE, 1980) recommends applying low-pass 4-th order Butterworth filters to crash dummy and test vehicle signals before extracting injury assessment parameters or determining the severity of impact. Each filter is designated by a "channel filter class" which is a number equal to 0.6 times its corner frequency. The corner of the filter is the frequency at which the power of the signal is attenuated by one half, i.e., where the magnitude of the filtered signal is -3 dB below that of the unfiltered signal. The filters recommended for filtering impact signals and computer subroutines for the design and implementation of digital Butterworth filters are listed in Appendix D.

Injury assessment

The two manikins used in the blast impact were Hybrid III type adult manikins for which injury assessment reference values are well established and accepted (Mertz, 1984; Ripple and Mundie, 1989). Although the reference values are derived from known human tolerance threshold values, the two are not the same since a reference value reflects the structural characteristics of a mechanical model. Further, the reference values used with a Hybrid III type manikin may not be valid for a different type of manikin, because the two types almost certainly will have different mechanical structures which produce different dynamic response to the same input.

Head injury commonly is assessed using the head injury criterion (HIC) when a direct impact to the head occurs. The HIC is a weighted impulse criterion which is derived from the resultant of the triaxial head acceleration sensor (FMVSS 208) (NHTSA, 1993) . Generally, it is implied that direct impact has occurred when the duration of the HIC was found to be less than 15 ms. The accepted reference value for a mid-sized male Hybrid III type manikin is 1000,

which corresponds to a 16 percent risk of life threatening brain injuries. An HIC value of 1500 is associated with a 55 percent risk of brain injury (Mertz, 1993).

Axial loading of the neck, which is measured by a single load cell, may be in compression or in tension. Injury assessment for compression is different from that in tension and from shear loading. Figure 1 presents the assessment curves for most types of neck loading (Mertz, 1993). The fore/aft shear curve is used also for lateral shear load assessment. Note that a given load must be sustained for the indicated duration. For neck flexion, a reference value of 1680 pounds-inches is used as the limit for neck bending moment, beyond which serious neck injury is likely.

Chest injury is assessed based on the resultant chest acceleration, measured at the center of gravity of the upper torso of the manikin. A resultant chest acceleration greater than 60 G is likely to cause serious thoracic injury, except when the resultant exceeds the 60 G threshold for intervals totaling less than 3 milliseconds (FMVSS 208) (NHTSA, 1993)

Injury assessment to the lower back (lumbar spine) is assessed from the lumbar load cell signals and from the seat acceleration signals. In mine blasts where a subject is restrained from excessive forward bending, the primary loading of the spine is the vertical direction. Human tolerance values and assessment methods for this type of loading, i.e., primarily axial loading of the lower spine in compression, are well established.

The Federal Aviation Regulation 29 (FAR, 1993) requires the axial compression force measured between the pelvis and the lumbar spine not to exceed 1500 lb for an aircraft seat to be considered safe. Because this number was derived in the early 1970s from tests with an older population of cadavers, a slightly higher threshold of 1800 lb has been suggested for the population of young adult Army pilots, and has been used by the Army for evaluation of OH-58 crashworthy seats (Haley and Palmer, 1994).

Other helicopter energy-absorbing seat designs have been based on limiting the seat acceleration to 14.5 G during purely vertical dynamic testing of crashworthy seats (Desjardins et al, 1989; and MIL-S-85510).

The U.S. Air Force uses the accelerations of ejection seats to compute the dynamic response index (DRI) and sets limits for the DRI for safe ejection seat operation (MIL-S-9479C). The DRI represents the maximum dynamic compression of the vertebral column of the human body. The equation defining the DRI and the limits used to assess the severity of multiaxis loading of the lumbar spine are defined by the Air Standardization Coordinating Committee (ASCC, 1989). High, moderate, and low injury risks (50, 5, and 0.5 percent probability of injury) have been assigned to DRI levels of 22.8, 18, and 15.2, respectively, derived from compressive ($+G_z$) accelerations. DRI limits for lateral (G_y) and fore/aft (G_x) accelerations also are assigned with less confidence because of lack of epidemiological data.

Velocity and displacement

In the absence of high-speed video or film record, velocity of the truck and, with less accuracy, its displacement, may be estimated by numerical integration of acceleration signals. Accelerometers mounted on the truck measure the motion of the mounting structure during the blast. The computed motion may be considered as the gross motion of the truck only if the structure and the truck frame move as a single rigid body. Unfortunately, this rarely is true because of structural flexibility of the truck frame. Therefore, accelerometers mounted on relatively lightweight structures, such as the truck bumper, should not be used to estimate the truck motion. In this report, truck cabin acceleration signals appear to be from well protected and solidly mounted transducers and will be evaluated.

Signal processing

Transducer signals recorded during the 8 December 1994 mine blast (test 120894) were converted to digital signals and delivered to USAARL for analysis. The signals were from triaxial accelerometers and load cells mounted in the two manikins, and included triaxial acceleration signals from the truck cab, bumper, and passenger seat.

The acceleration signal data acquisition system provided 10,000 samples per second (10 kHz) per channel as recommended in J211 guidelines for manikin impact signals. A total of 1000 milliseconds (100 ms pre- and 900 ms posttrigger) were digitized; however, only 900 ms were provided and, eventually, only 500 ms were considered for analysis. An attempt was made to identify the appropriate polarity of each signal. After careful examination of the results, it was not possible always to confirm the polarity of all signals; however, their magnitudes were considered to be valid. The reduced-size and uniformly filtered signals from the test then were compressed in a single binary file which was used as input for further processing. Following zero adjustment and appropriate filtering, the triaxial signals were used to derive the appropriate injury assessment parameter, e.g., dynamic response index (DRI) or head injury criterion (HIC), or simply plotted at time histories for evaluation.

Results

The raw signals, i.e., unadjusted, unfiltered, are plotted in Appendix A. The plots include the first 400 ms of posttrigger data and a 50 ms pretrigger segment. Plots in this appendix are grouped in triaxial sets reflecting the location of the transducer. This raw display was necessary to identify lost and invalid signals which were not used in the assessment. Clearly, the bumper accelerometers, the driver head, and chest accelerations were unusable for injury assessment. Truck cab acceleration in forward direction also was lost and was not analyzed.

The remaining acceleration and force signals were considered to be valid and, after appropriate zero adjustments and filtering, were used for evaluation of the passenger seat and manikin response, and for comparisons between the manikin responses. The filtered and zero-adjusted signals from all transducers are contained in Appendix B, including signals which were not valid for analysis.

Truck and EA passenger seat motions

Truck motion was estimated from the processed cabin floor accelerations and velocities, shown in Figures 2 and 3, respectively. The primary impact occurred between 15-20 ms after the blast and reached 119 G in the vertical direction, and 50 G in the lateral direction. The vertical velocity, obtained by integration of cabin floor vertical acceleration signal, reached its peak of 19.4 ft/sec at about 22 ms posttrigger. After 80 ms, the velocity appeared to return to zero. Of course, a zero vertical velocity (not its peak) indicates that maximum height was attained and the truck will reverse direction and fall back to the ground.

Figure 4 shows 100 ms window of accelerations of the EA passenger seat in the forward (G_x), lateral (G_y), and vertical (G_z) directions. Peak seat accelerations were 53 G_x, 39 G_y, and 43 G_z, and occurred in the first 30 ms after the blast. The vertical acceleration (top curve, Figure 4) reveals the wire bending action of the passenger seat as it absorbs energy. No data from the standard (driver) seat were available for comparison. Because the EA seat accelerations were not measured at the seat reference point (SRP), no dynamic response indexes were computed for the passenger seat. Instead, an indication of the impact received by the seat may be estimated from the velocities at the seat pan. The velocities of the EA seat, obtained by integrating accelerations, are shown in Figure 5. The greatest velocity occurred in the vertical direction and measured 21.6 feet per second.

Passenger pelvis accelerations

Accelerations at the pelvis of the passenger manikin are shown in Figure 6. Peaks of the initial pulses of the acceleration signals were 85 G_x, 38 G_y, and 42 G_z, all of short durations (under 5 ms) occurring within the first 10 ms after the blast. Peaks of longer pulses (20-30 ms) occurred approximately 25 ms postimpact and measured 43 G_x, 8.9 G_y, and 32 G_z. Since the center of mass of the pelvis coincides with the SRP of the EA seat, it was appropriate to compute the DRI from the G_x, G_y, and G_z accelerations of the pelvis. The DRI values were 12.2 G_x, 3.8 G_y, and 16.6 G_z.

Head and chest accelerations

Figure 8 shows the triaxial accelerations measured at the head center of gravity of the passenger manikin. The peak resultant head acceleration was 192 G and occurred at 5 ms post-trigger. This acceleration level was not due to any direct contact with objects in the cabin, but is due to the forces transmitted to the head through the stiff structure of the neck and upper torso. A level of 70 G sustained for 3 ms has been used in evaluating helmet impacts. The cumulative duration of resultant above 70 G was estimated to be less than 2 ms. In addition, the head injury criterion was computed (HIC = 79) for the passenger manikin. This value is associated with no risk (0% probability) of life-threatening brain injury.

Driver's head accelerations clearly were invalid (see Appendix A) due to apparent instrumentation failure, so that no comparison between the two manikin head responses were possible. Comparison of thoracic responses of the two manikins or assessment of chest accelerations of either manikin also were not possible because of lack of data or its invalidity.

Spinal column forces

The spinal column forces in the driver (unmodified seat) and passenger (EA seat) manikins are presented in Figures 9 and 10 for the cervical spine (neck), and in Figures 11 and 12 for the lumbar spine (lower back). Neck forces were filtered at 300 Hz, and lumbar forces at 100 Hz to highlight the primary peak of the compression force. In all force signals, the initial spikes, designated as "Peak 1," occur at about 3 ms postimpact, have very short (less than 2 ms) durations. The primary pulses, whose peaks are designated as "Peak 2," occur 25-30 ms post-impact, have longer durations (greater than 20 ms). A comparison of the peaks, extracted from Figures 9-11, is presented in Table 1.

As expected, the highest force occurred in the vertical direction, i.e., in axial compression in both occupants. Peak axial compression forces of the cervical spine (neck) were 333 lb for the driver and 383 lb for the passenger. The polarities were not clear from the information supplied with the data. However, it is safe to assume the high peak was in compression because the impact of the blast was in the upward direction. Again, because the impact primarily was in the vertical direction and along the spinal axis, the forces in axial compression were highest in both manikins. Peak lumbar forces were 2159 lb for the driver and 1329 lb for the passenger. A noteworthy result is the fore/aft shear force in the passenger lumbar spine, which reached 782 lb.

Table 1.
Comparison of peak spinal forces at the cervical (neck) and lumbar (lower back) regions in driver and passenger manikins.

		Fore-aft shear Fx (lb)		Lateral shear Fy (lb)		Axial compression Fz (lb)	
Location	*Manikin*	*Peak 1*	*Peak 2*	*Peak 1*	*Peak 2*	*Peak 1*	*Peak 2*
Cervical (neck)	Driver	-919	-75	-942	-9.4	-1119	**-333**
	Passenger	-188	-65.7	-48.7	21.5	-352	**-383**
Lumbar (back)	Driver	-135	246	-274	-153	-734	**-2159**
	Passenger	-427	**-782**	-433	-50.2	-1171	**-1329**

Discussion

An examination of the raw data is essential to weed out invalid signals that were lost due to unforseen hardware and instrumentation problems. After the appropriate zero adjustment and filtering are applied to the valid signals, the produced signals may be considered as accurate measurements of the truck and manikin accelerations and forces. Of the 33 signals (11 triaxial sets) which we received, we found 10 signals were unusable. The remaining 22 signals were judged to be valid and usable after appropriate processing.

Truck motion

Despite all the precautions taken to firmly mount accelerometers to heavy and solid structures, high frequencies that have no relevance to the gross motion of the truck always will be present in the acceleration signals. This implies that filtering is necessary and must be done to remove the undesired (and irrelevant) high frequencies from the signal. Shock mounting of the transducer on a soft pad attached to the vehicle will produce a noise-free signal because, in effect, the underlying vehicle acceleration is being mechanically filtered. This may be necessary to protect the accelerometer from excessive signals and prevent signal clipping.

A balance between the desire to protect the instrumentation hardware and the need to avoid total distortion of the signal usually is achieved by trial and error and draws from prior experience in shock testing of a given vehicle. Even when the transducer mounting method was

adequate, the bumper was not the proper location to observe the gross motion of the truck, but reflected only the high frequency and high magnitude structural resonances of the relatively lightweight bumper structure. This caused failure of the instrumentation of all three accelerometers, as may be observed in Figure A-1 of Appendix A. The truck cabin was reinforced and was less likely to deform. Therefore, accelerometers mounted on cabin structures were more indicative of the gross motion of the truck than bumper accelerometers, and should be used to estimate a velocity and acceleration of the truck. The relatively low accelerations measured at the cabin are attributed to the blast protection deflector which diverted the thrust of the blast from being applied upward to the cabin and its occupant.

EA seat motion

Accelerations at the seat of the truck occupant (driver or passenger) are more relevant than cabin acceleration signals because they describe the input received by the occupant. For this reason, seat accelerations should be specified as input to crash simulations, such as the articulated total body (ATB) model. Figures 4 and 5 are included to provide realistic and accurate specifications of the input to such models when simulating an energy absorbing seat. No similar data was available for the driver seat.

The results obtained after appropriate signal processing show that no seat accelerations (nor pelvis, nor truck cab accelerations) ever reached 100 G. Accordingly, simulations and assessments based on an assumed acceleration pulse having a 3-ms plateau of 100 G magnitude should not be considered as representative of the 120894 mine blast test.

All three accelerations of the passenger seat were valid signals. A close up of the first 10 ms, shown in Figure 4, indicates the first peaks (approximately 40 G in all directions) occurred almost simultaneously at about 6 ms postimpact. The vertical acceleration did not return to zero until 25 ms later, indicating the wire bender was doing its job absorbing impact energy. This is the "acceleration" phase of the seat motion, as indicated by the rising portion in the vertical velocity curve of Figure 5. After the EA seat reaches a peak velocity of 21.5 ft/s, it slows down and comes to rest approximately 100 ms postimpact.

Although the DRI usually is associated with seat accelerations, none was calculated from the EA seat accelerations since they were measured at the seat pan bottom and not at the seat reference point (SRP). More appropriately, the DRI was derived from pelvis accelerations (as discussed later) since the pelvis center of mass approximates the SRP.

Head acceleration

The sharp initial peaks are due to the stiff structure of the manikin which was designed primarily for frontal impacts. No evidence of direct head impacts were found, indicating the

success of the tested mine protection kit in preventing head impacts and subsequent brain injuries.

Pelvis accelerations

Although the same 100-Hz filter was applied to the accelerations measured at the passenger seat (Figure 4) and at the passenger pelvis (Figure 6), differences were observed. One explanation for the difference between seat and pelvis accelerations is that the pelvis mass was much less than the seat mass, so dynamic magnification was likely to occur when energy was transmitted from the seat to the manikin. This phenomenon is common and usually is described as a "dynamic overshoot." In this case, based on the peaks of vertical accelerations between the seat (28 G) and pelvis (42 G), the dynamic overshoot is 42/28 or 1.5 factor. In dynamic sled tests, dynamic overshoot factors typically range from 1.0 (i.e., none) at the pelvis to 2.5 at the head.

Another explanation is the coupling between pelvis and seat was not as tight as desired. The excessive forward pelvis acceleration of the passenger manikin indicates the seat belt may not have been properly tightened, or the manikin was not seated firmly in the seat. This assertion is supported by the lack of forward acceleration of the seat itself, the lack of lateral pelvis motion, and the readings of the lumbar spine forces which also indicate excessive fore-aft shear.

One of the predictors of lumbar spine injury is the DRI which is based on accelerations measured at the SRP that coincides with the center of mass of the pelvis. Therefore, pelvis accelerations, shown in Figure 6, are the appropriate signals for DRI computations and injury prediction. Thus, the DRI of passenger pelvis (Figure 7) were 13.38 G_x, 3.81 G_y, and 15.21 G_z.

Since the DRI in the vertical direction was the largest, we examined it for injury prediction. High, moderate, and low injury risks (50, 5, and 0.5 percent probability of injury) usually are assigned to DRI levels of 22.8 Gz, 18 Gz, and 15.2 Gz, respectively. Therefore, the EA seat produces compressive pelvis acceleration in the passenger which have a low injury risk. Based on passenger pelvis and seat accelerations, and on DRI prediction, we concluded the new seat EA design prevented transmission of excessive accelerative forces to manikin, and would have prevented serious spinal injuries to the occupant of the truck in a mine blast.

Cervical spine (neck) forces

The forces of the upper neck joint were highest in compression (vertical direction) for both driver (333 lb) and passenger (383 lb). Both values exceed the 250-lb limit generally accepted as the neck injury threshold. However, the appropriate injury assessment criteria (Figure 1) take into account the duration of the application of the force. To assess the injury potential of neck compressive forces, the primary neck compression pulses in the passenger and driver manikins, which occurred between 20 and 50 ms postimpact, were re-plotted in Figure 13. Clearly, neither of the manikins neck compressive forces exceeded the threshold of 250 lb for more than 17 ms,

about half the duration required to trigger serious neck injury at this load. Therefore, injury to neck in both manikins were not likely to have occurred.

It is worth noting, however, that neck compression force in the passenger manikin was 15 percent higher than that in the driver. Since no data were available on driver manikin chest, pelvis, or seat accelerations, it is not clear whether this outcome was an unavoidable consequence of the EA seat design or the result of loose lap belt and poor seating of the passenger. Given other indications (unusual fore-aft pelvis motion and forces), and the reduction in lumbar forces, it is not likely the EA design was responsible for this aberration.

Lumbar spine (back) forces

Compressive forces in the lumbar area of the spine were highest in both manikins: 1329 lb for the passenger and 2159 for the driver. These results suggest the EA seat achieved design goal of reducing forces transmitted to lower spine, in this case, by about 38 percent. Also, it seems appropriate to apply the threshold of 1500 lb as the assessment reference value, and to conclude the EA seat (passenger) would have prevented serious lower spinal injuries, whereas the standard seat (driver) would not. Although the threshold of 1500 lb is specified for any pulse duration, a realistic criterion would account for pulse duration above the threshold. Unfortunately, no such criterion has been validated or accepted by the injury assessment community.

Conclusions

1. The blast deflectors, part of the NVESD mine blast protection kit, reduced upward accelerations of the truck cabin and, subsequently, vertical input to the seated occupants.

2. The cabin floor reinforcement and occupant restraint system, part of the NVESD mine protection kit, were responsible for absence of head contact (flail) injuries.

3. The energy-absorbing seat design, also part of the same mine protection kit, was responsible for reduced vertical lumbar spine forces by 38 percent.

4. It was not possible to make full injury assessment of lumbar spine of the driver seated in the unmodified seat.

5. Recommendations for improving the instrumentation and signal acquisition and analysis in future mine blast tests were provided.

References

Air Standardization Coordinating Committee. 1989. Six-degree-of-freedom evaluation method. ASCC advisory publication 61/66, 10 May 1989.

Department of Defense. 1981. General specification for seats, helicopter cabin, crashworthy. Washington, DC: Department of Defense. MIL-S-85510(AS). 19 November.

Department of Defense. 1993. General specification for seat system, upward ejection, aircraft. Washington, DC: Department of Defense. MIL-S-9479C(USAF). 20 October.

Desjardins, S. P., Zimmermann, R. E., Bolukbasi, O., and Merritt, N. A. 1989. Aircraft crash survival design guide. Fort Eustis, VA: U.S. Army Aviation Research and Technology Activity. USAAVSCOM TR 89-D-22D.

Federal Aviation Regulation. 1993. Airworthiness standards: transport category rotorcraft, Part 29. §29.562, Emergency landing dynamic crashworthiness, section (c)(7). Washington, DC: Federal Aviation Administration.

Haley, J. L., Jr., and Palmer, R. W. 1995. Evaluation of a retrofit OH-58 pilot's seat to prevent back injury. Fort Rucker, AL: U.S. Army Aeromedical Research Laboratory, USAARL Report No. 95-9.

Mertz, H. J. 1984. Injury assessment values used to evaluate Hybrid III response measurements. Washington, DC: National Highway Transportation Safety Administration. NHTSA Docket 74-14, Notice 32, Enclosure 2 Of Attachment I of Part III of General Motions Submission USG 2284. March 22.

Mertz, H. J. 1993. Anthropomorphic Test Devices. *Accidental injury: Biomechanics and prevention,* chapter 4. Alan Nahum, John Melvin (editors). New York: Springer-Verlag.

National Highway Traffic Safety Administration. 1993. Federal Motor Vehicle Safety Standard. FMVSS20849 CFR Ch. V (10-1-93 Edition), §571.208, S6.1.2 and S6.1.3.

Ripple, G. R., and Mundie, T. G., ed. 1989. Medical evaluation of nonfragment injury effects in armored vehicle live fire tests - instrumentation requirements and injury criteria. Washington, DC: Walter Reed Army Institute of Research. Report AD-A233-058. September 1989.

Society of Automotive Engineers. Instrumentation for impact tests - SAE recommended practice. Warrendale, PA: Society of Automotive Engineers. SAE J211 Jun80.

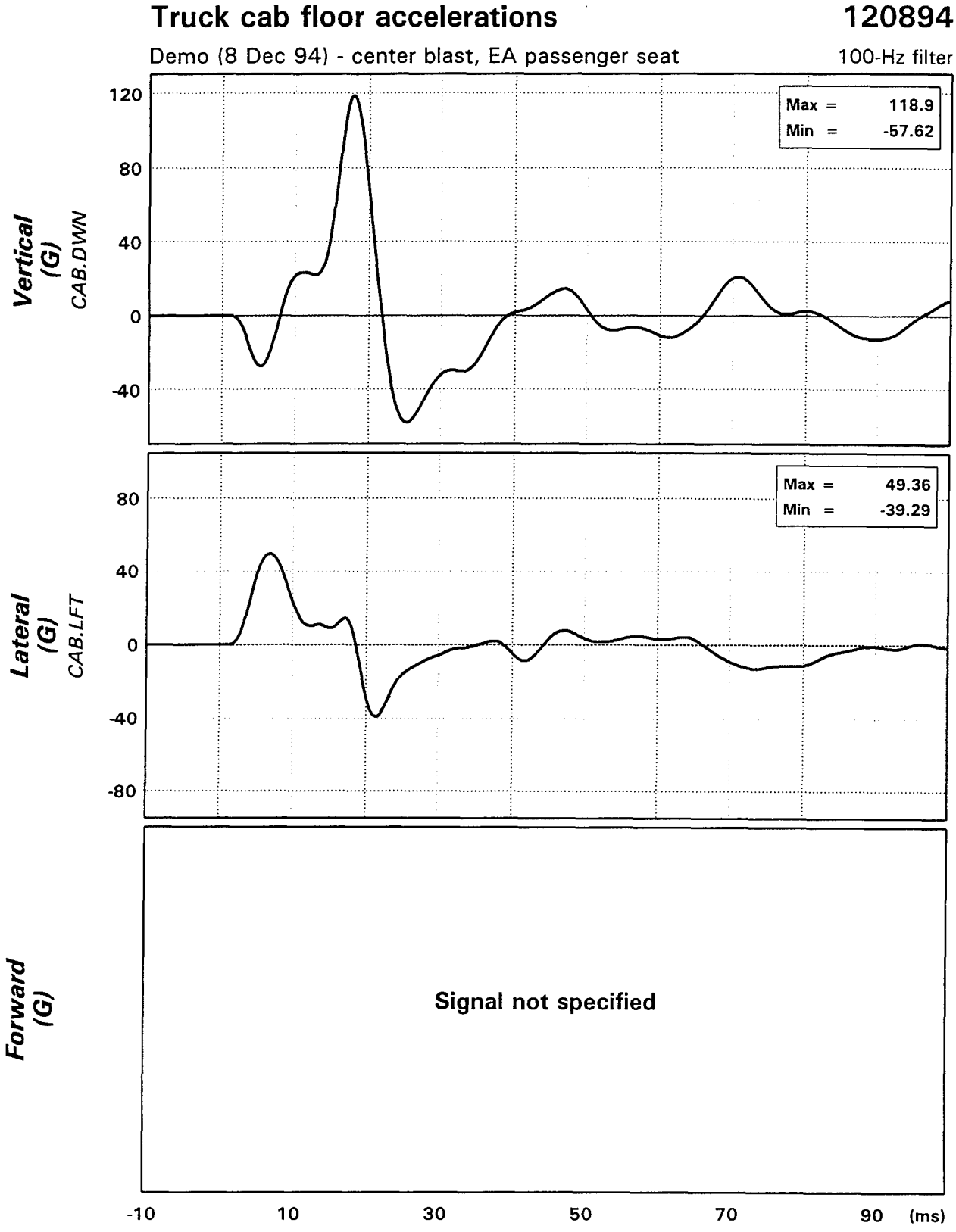

Figure 2. Accelerations of the truck cabin floor in the vertical and lateral directions. Forward acceleration signal was not available.

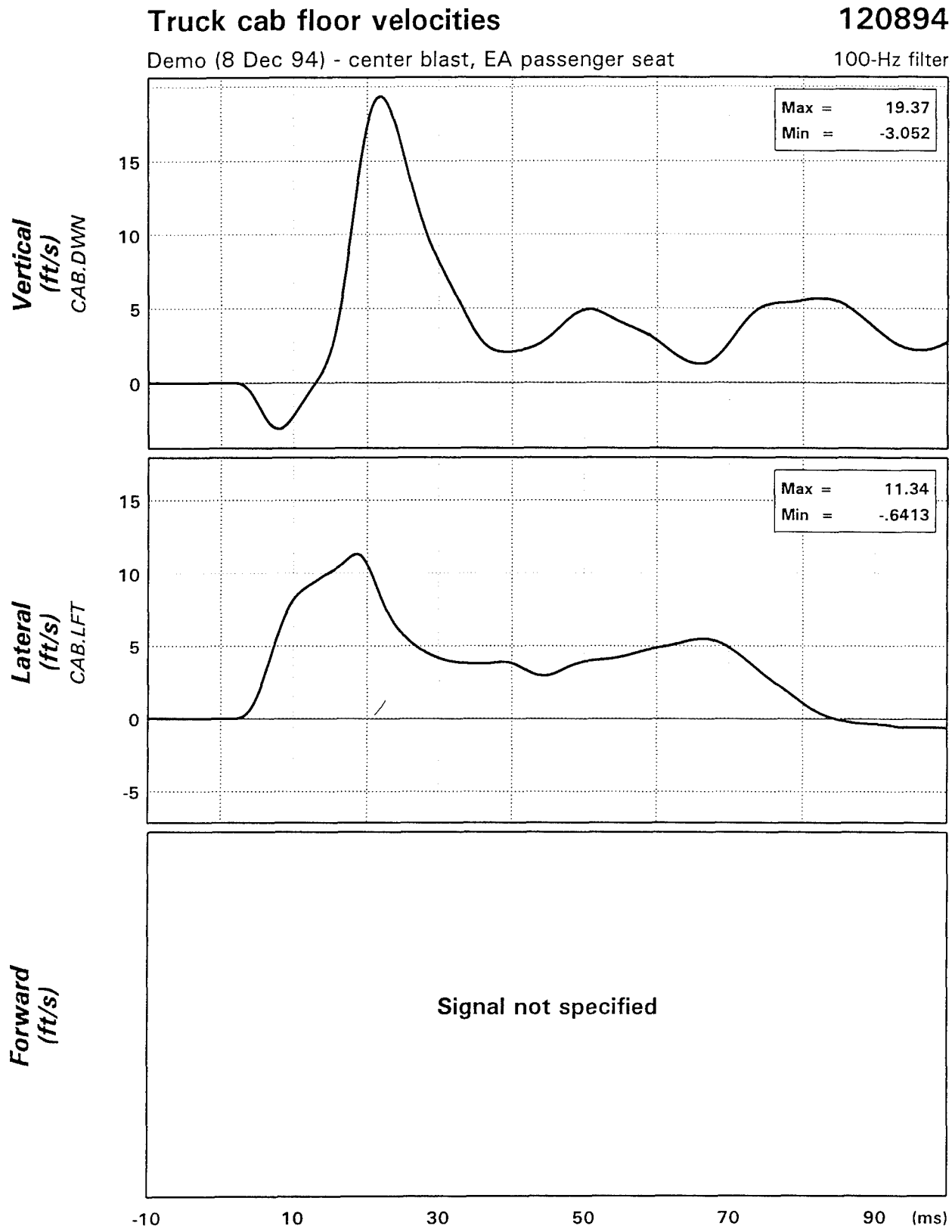

Figure 3. Velocities of the truck cabin floor in the vertical and lateral directions, obtained by integrating the processed acceleration signals.

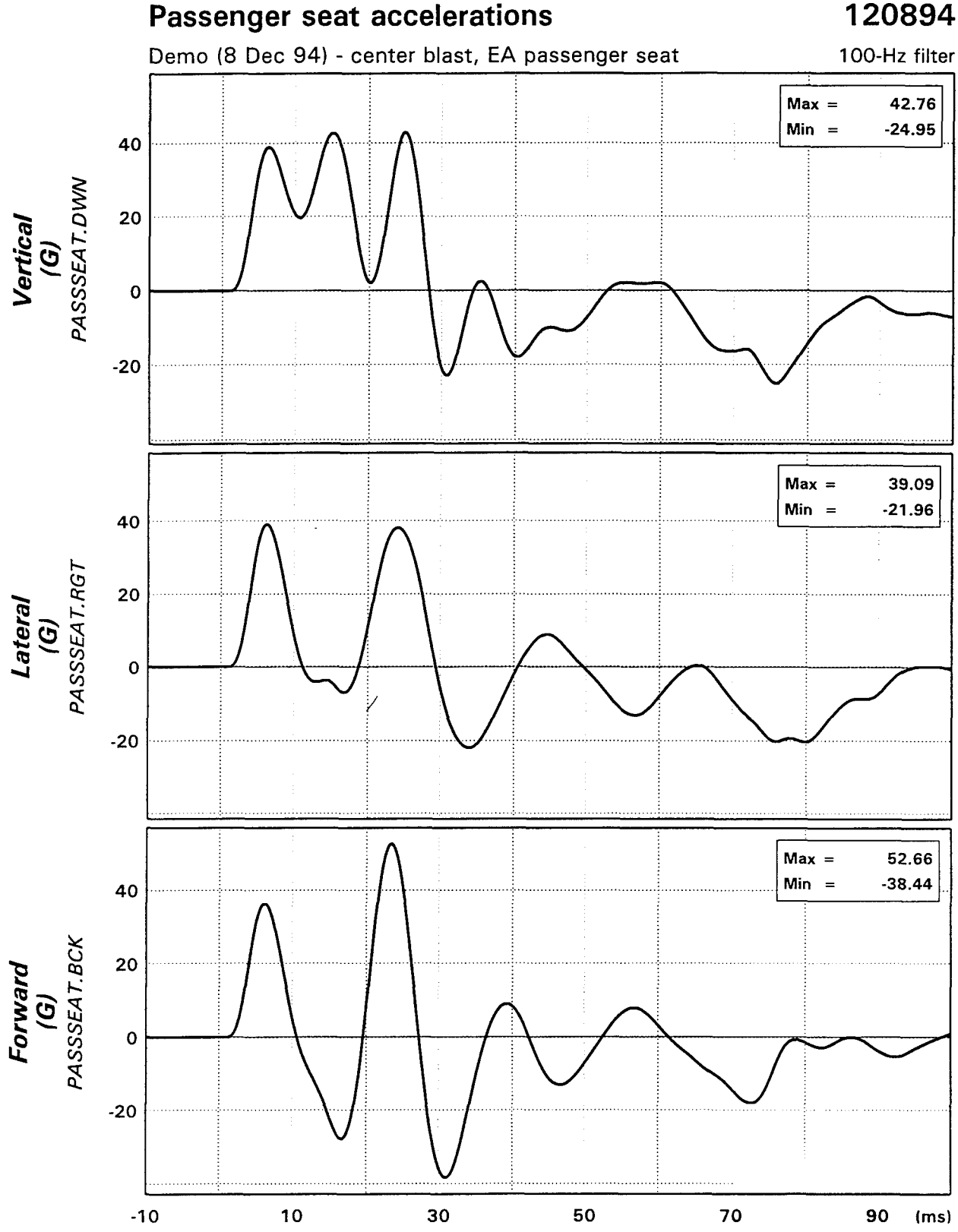

Figure 4. Triaxial accelerations of energy-absobing passenger seat. Vertical accelerations were limited by the wire bending action.

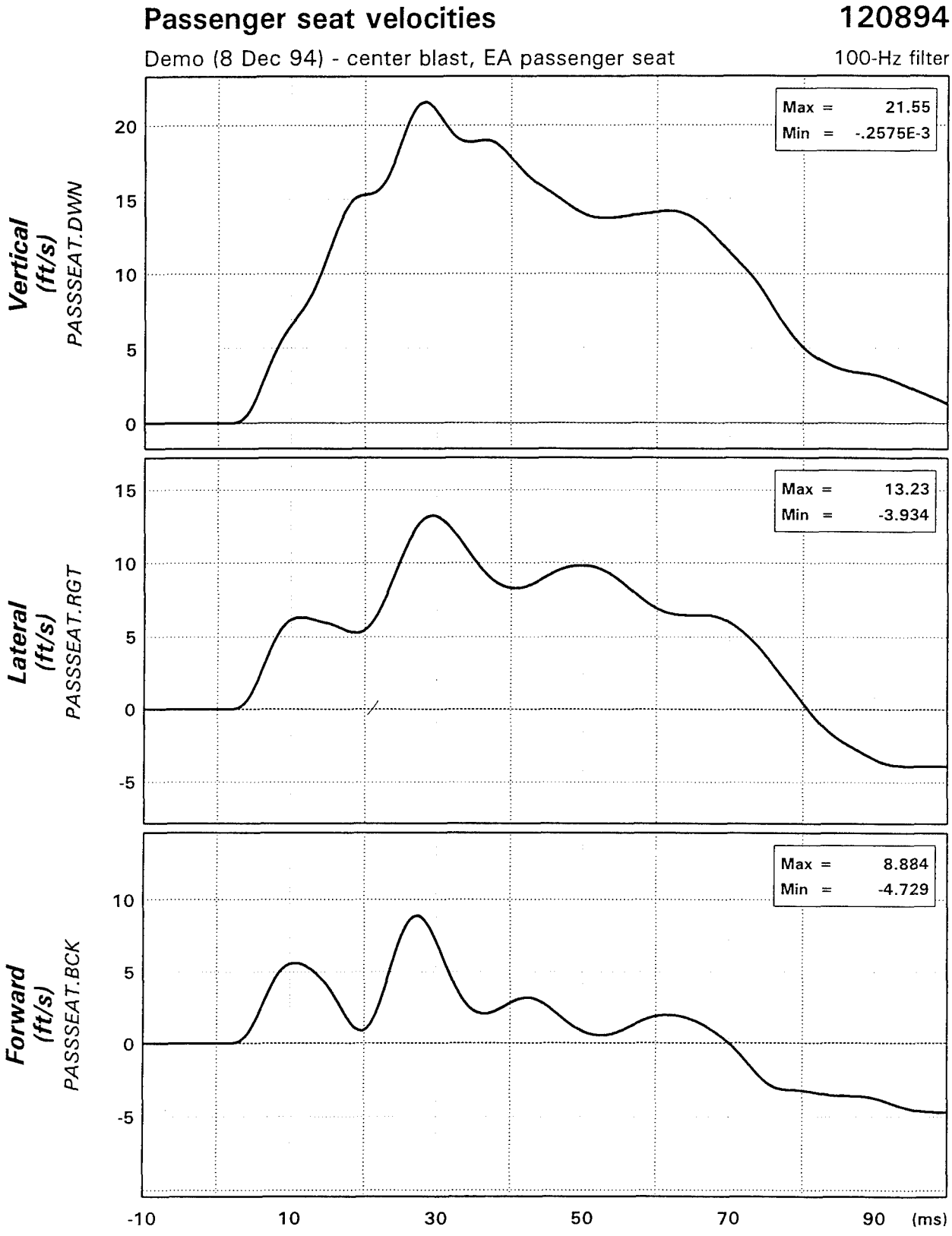

Figure 5. Velocities of the passenger seat, obtained as integrals of acceleration signals, assuming they return to zero near the end of the pulse.

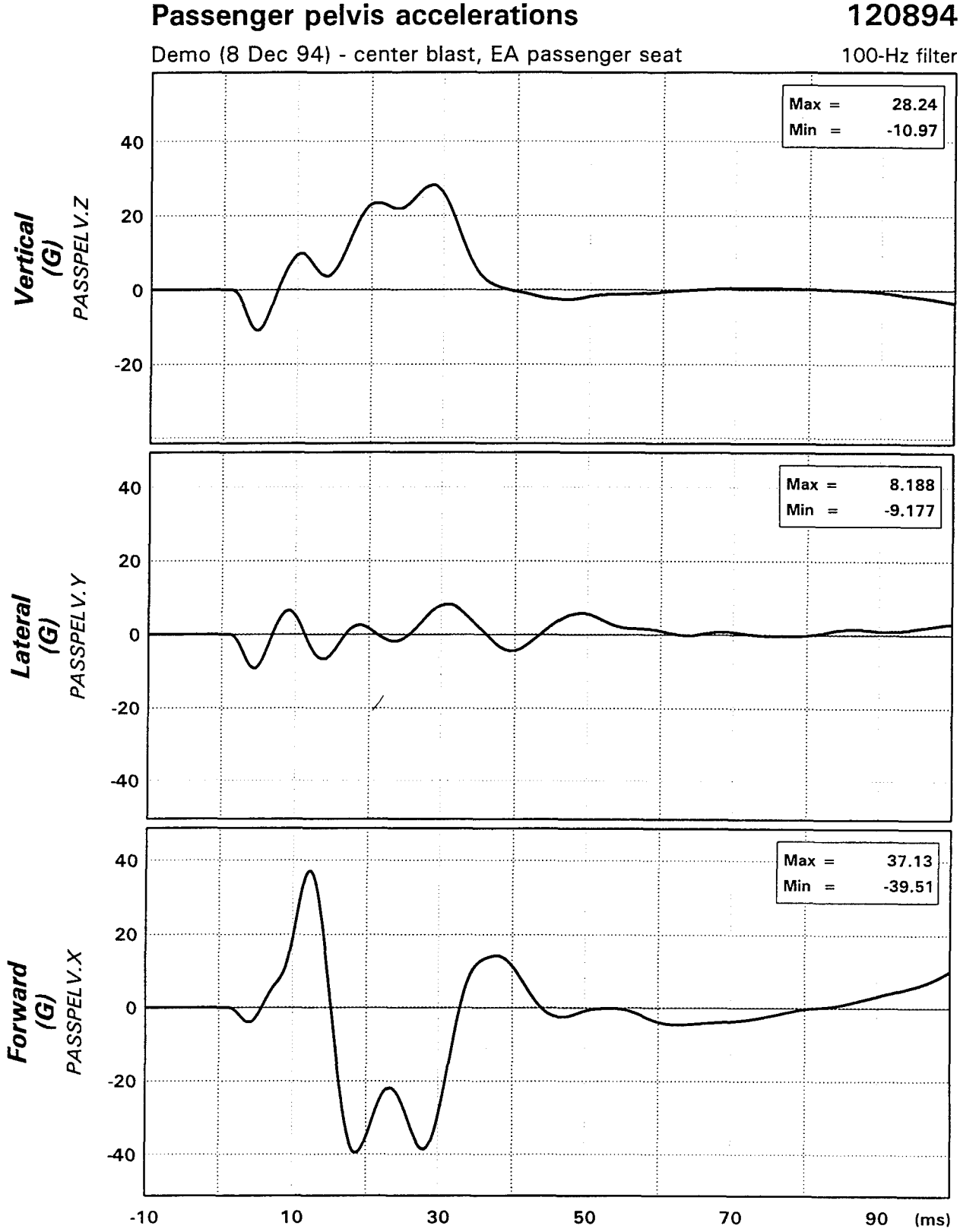

Figure 6. Passenger manikin pelvis accelerations which may also be considered measurements at the seat reference point (SRP).

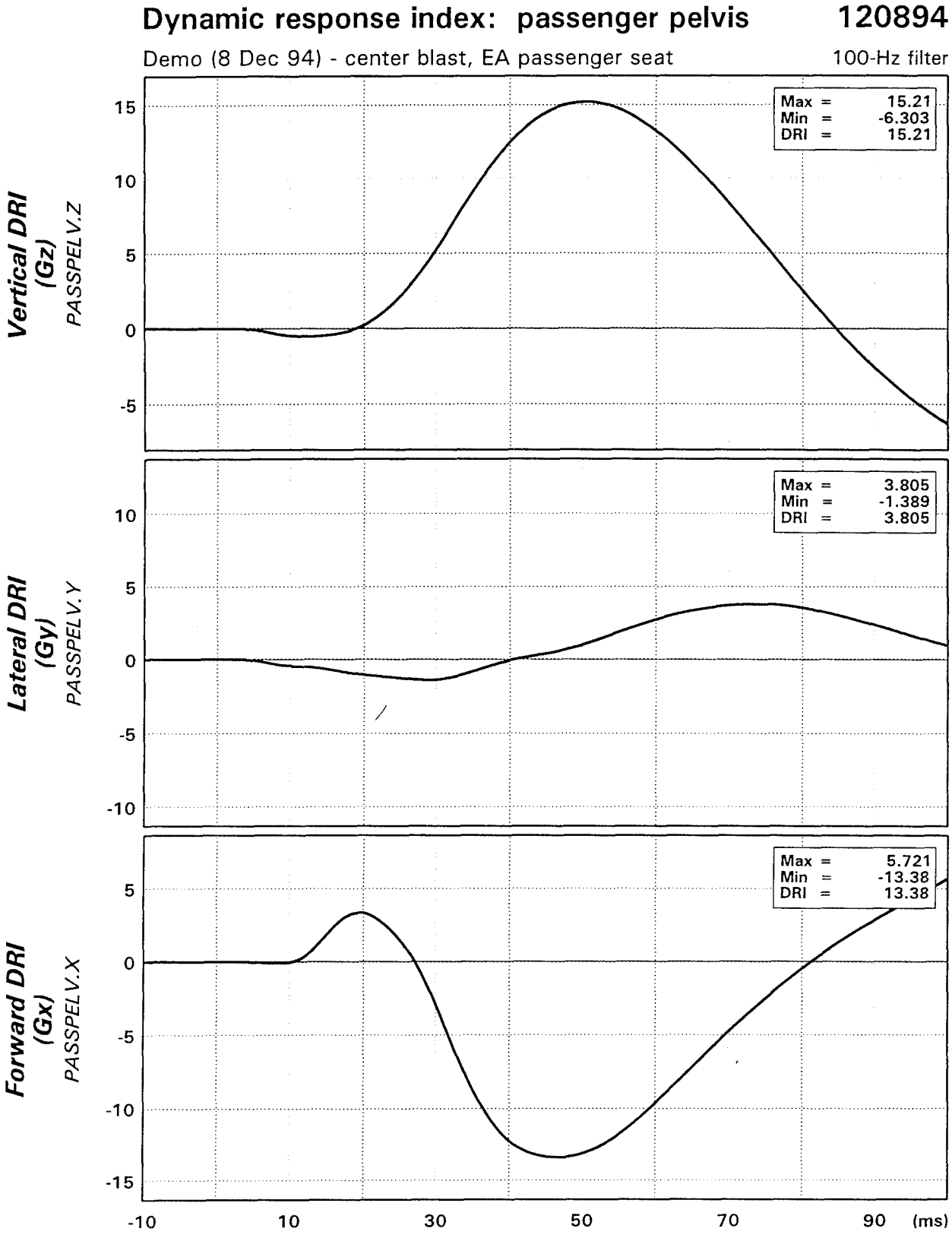

Figure 7. Dynamic response index (DRI) functions and peaks obtained from passenger pelvis acceleration signals.

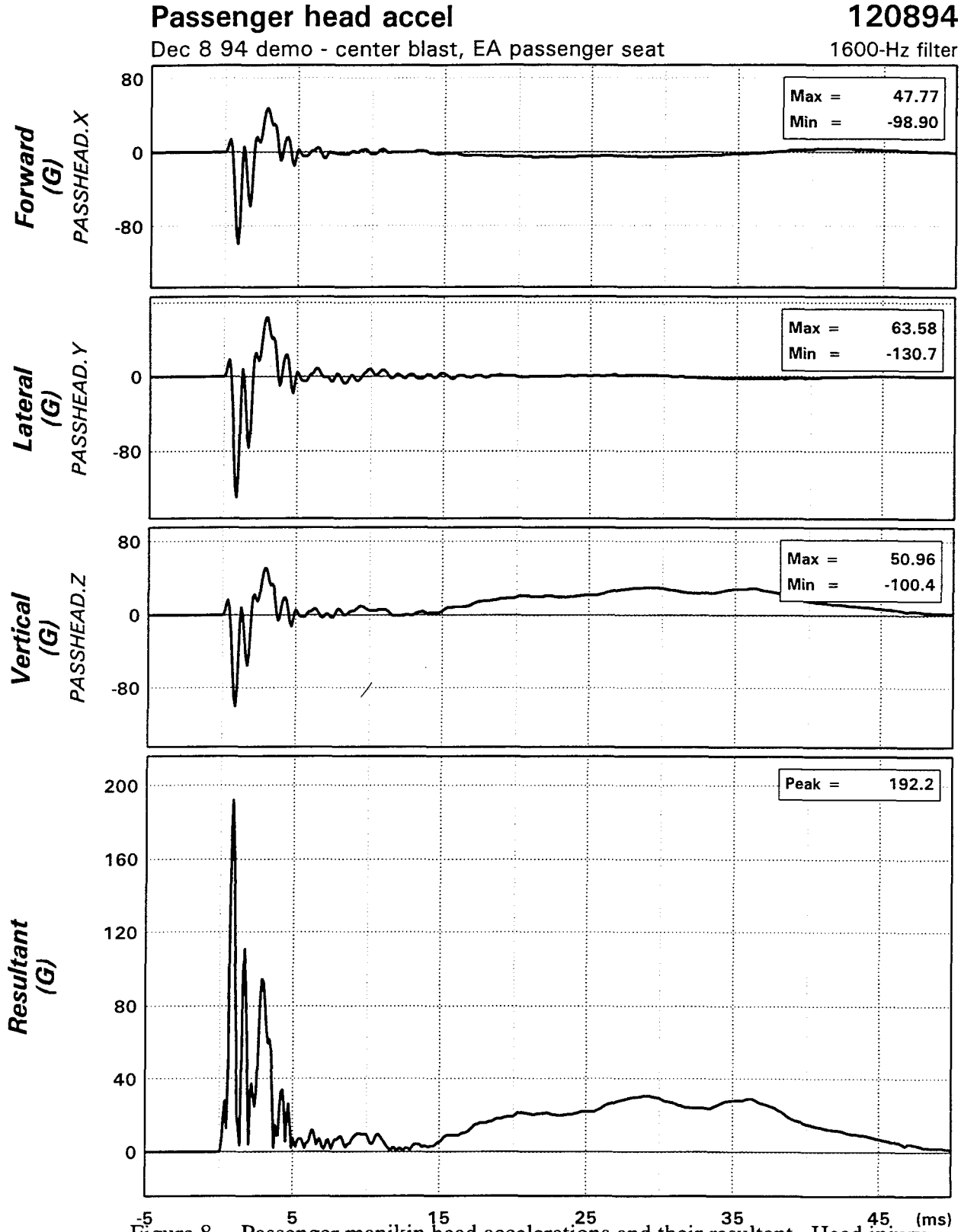

Figure 8. Passenger manikin head accelerations and their resultant. Head injury criterion did not predict serious brain injury.

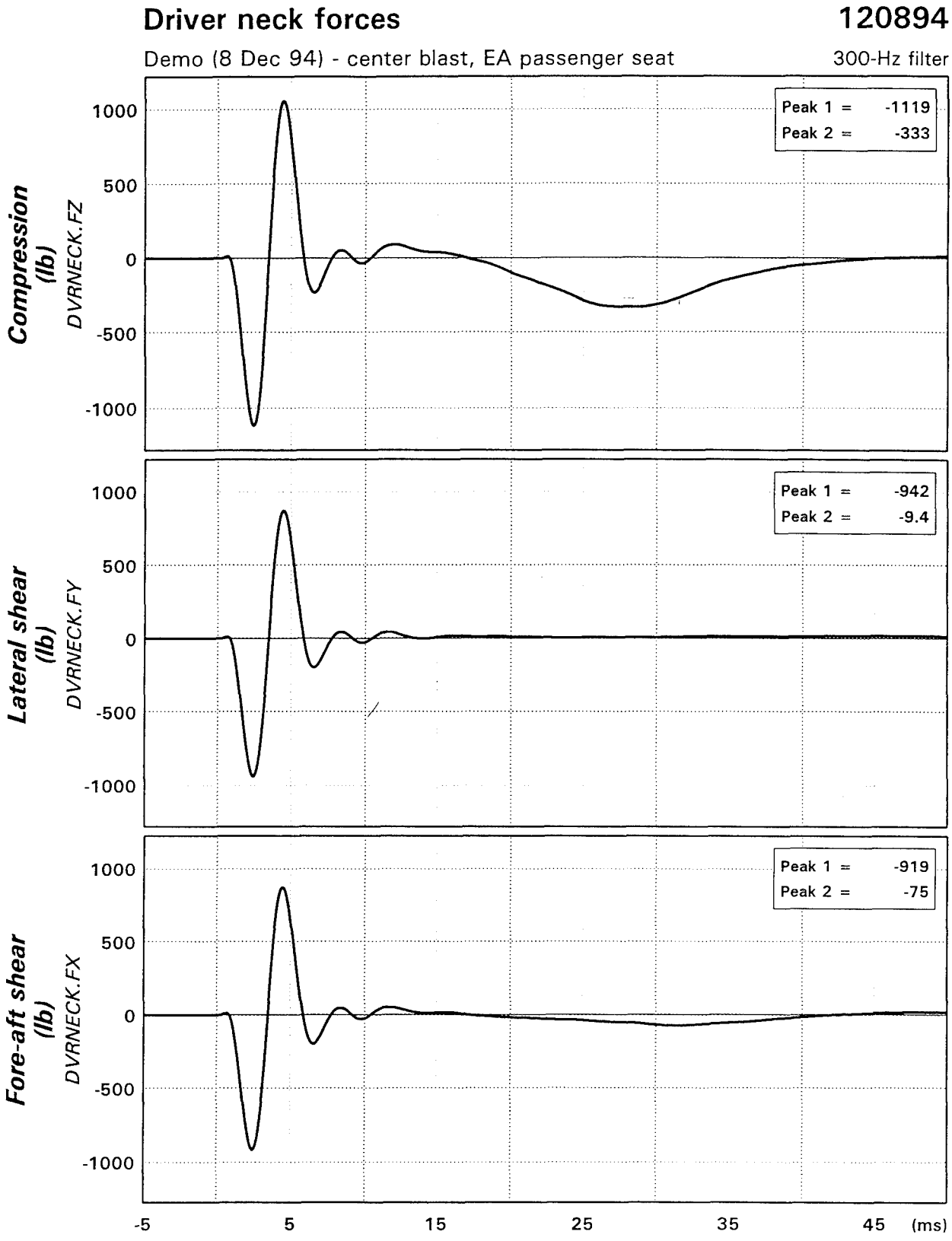

Figure 9. Driver manikin cervical spine (neck) forces in fore/aft and lateral shear and in axial compression/tension.

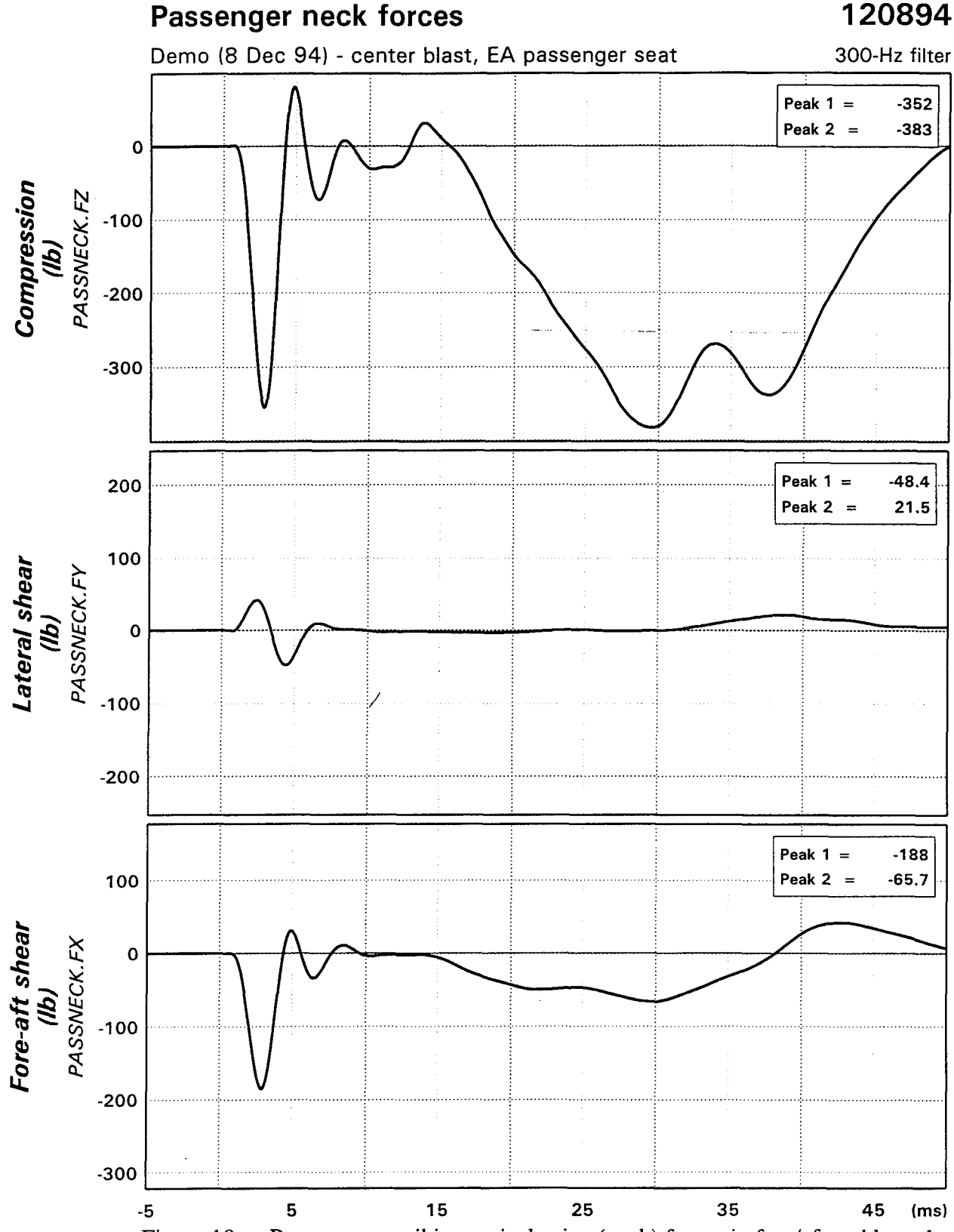

Figure 10. Passenger manikin cervical spine (neck) forces in fore/aft and lateral shear and in axial compression/tension.

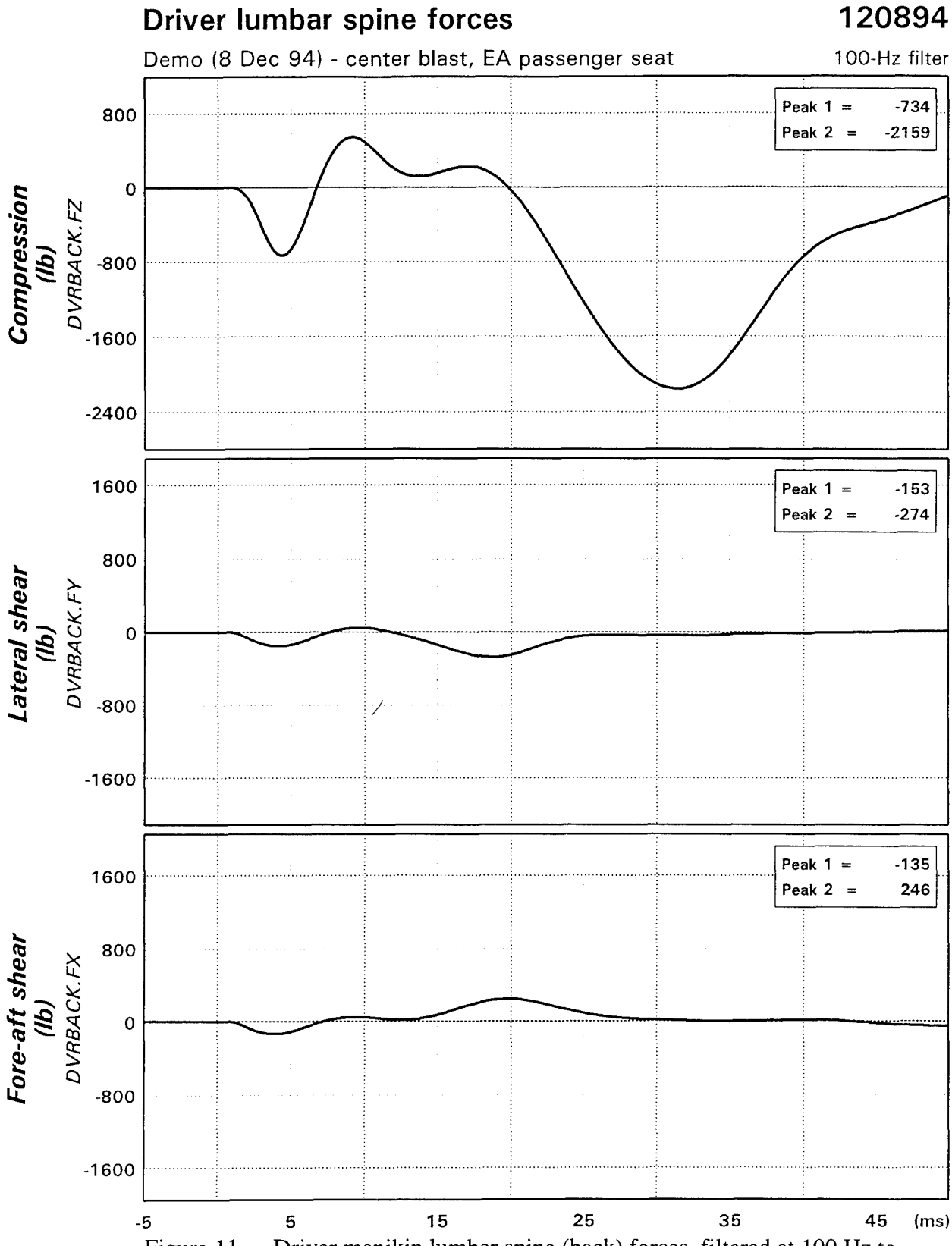

Figure 11. Driver manikin lumber spine (back) forces, filtered at 100 Hz to remove initial short-duration spikes.

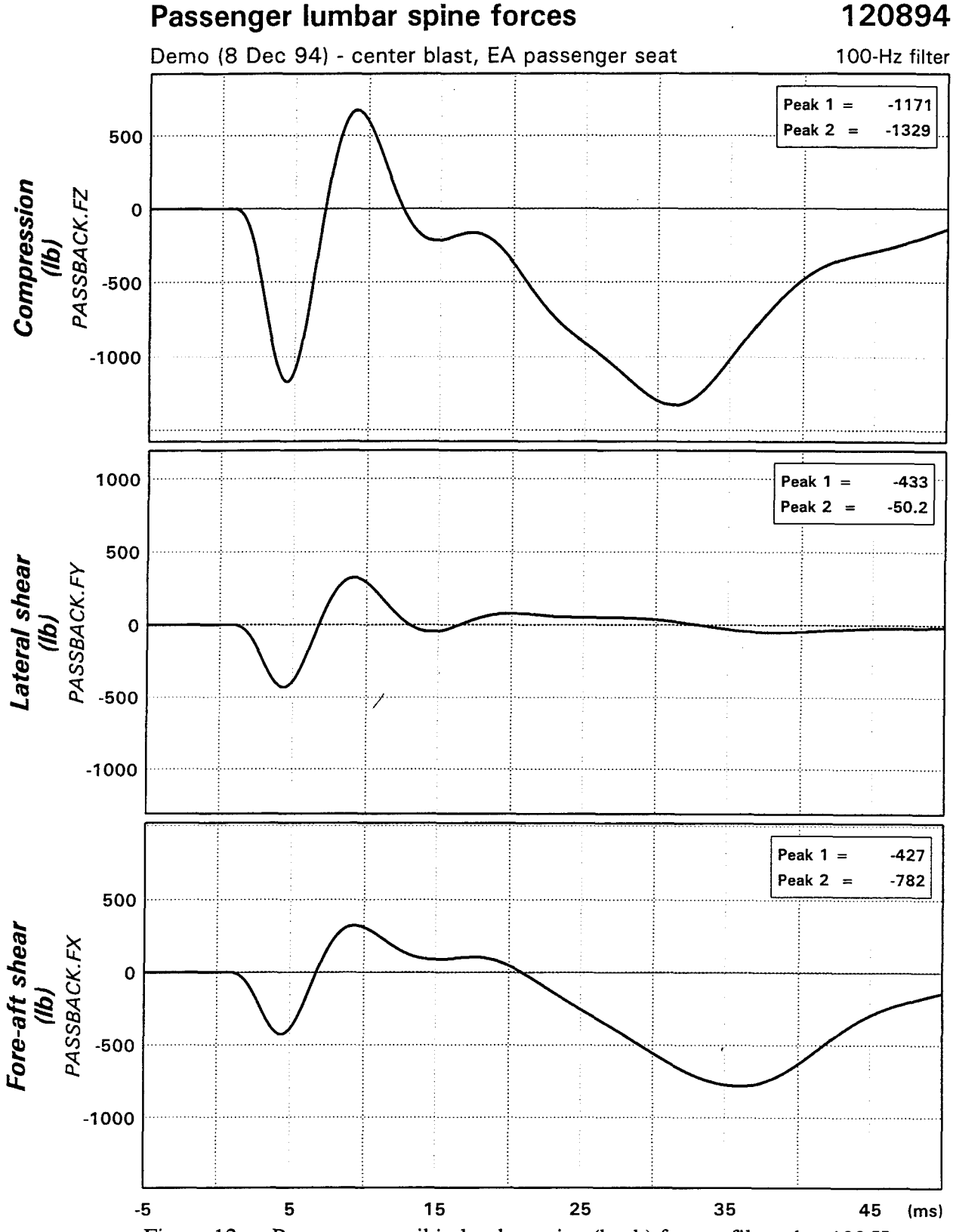

Figure 12. Passenger manikin lumbar spine (back) forces, filtered at 100 Hz to remove initial spike and highlight main peak force.

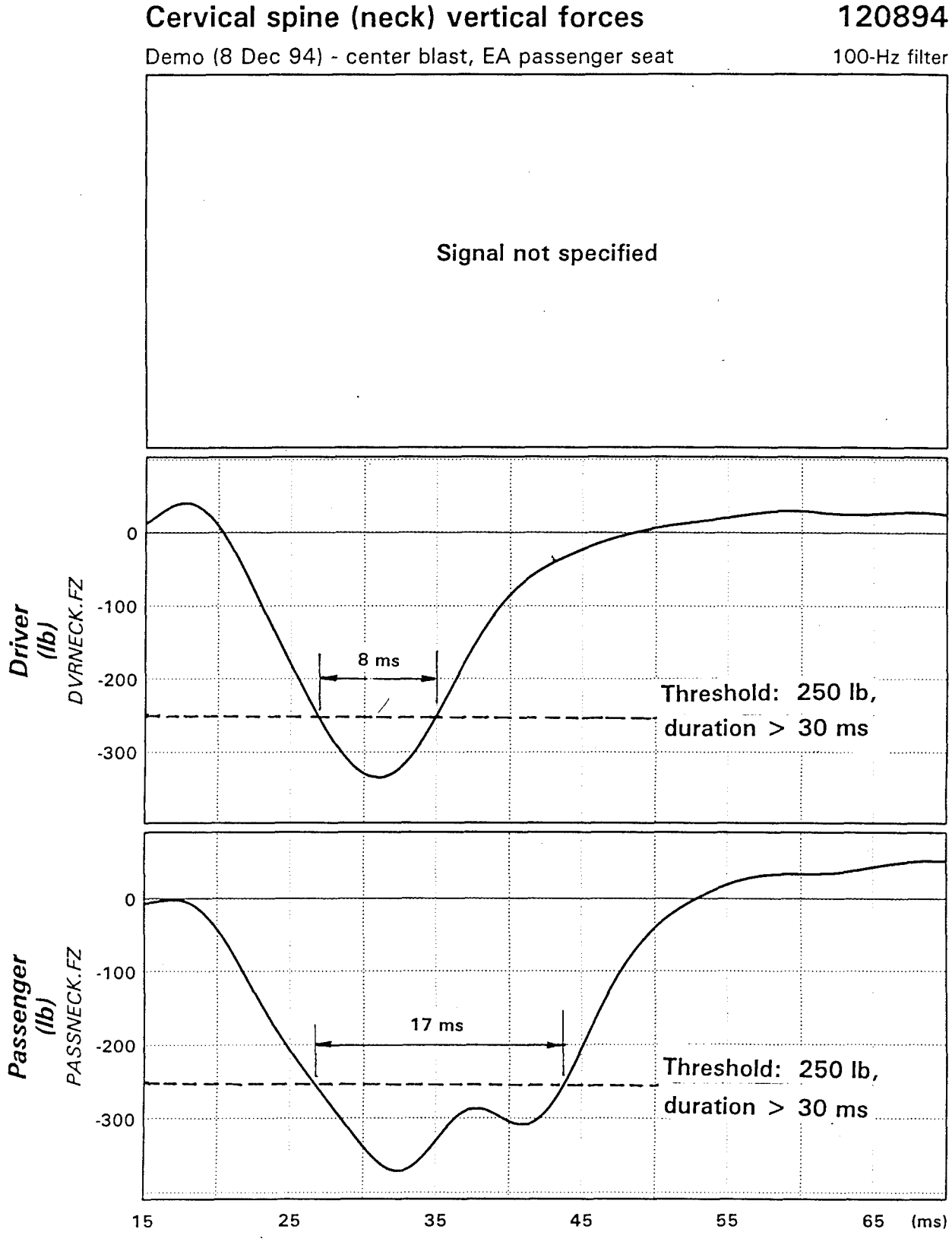

Figure 13. Injury assessment of cervical spine (neck) compressive forces.

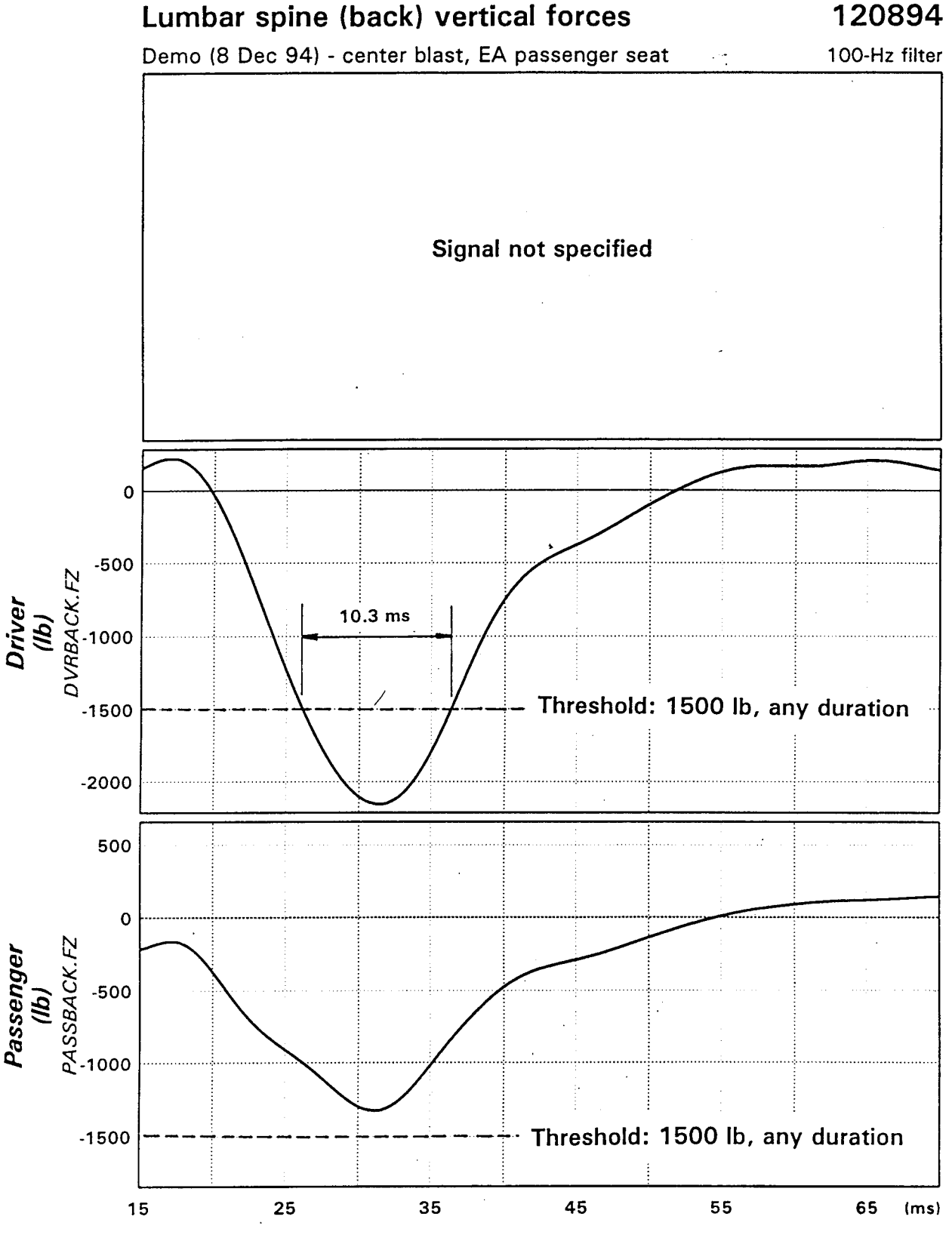

Figure 14. Injury assessment of lumbar spine (lower back) compressive forces.

Appendix A.

Raw transducer data of test 120894.

Transducer signals recorded during the 8 December 1994 mine blast test were converted to digital signals and delivered to USAARL for analysis. The signals were from triaxial accelerometers and load cells mounted in the two manikins, and included triaxial acceleration signals from the truck cab, bumper, and passenger seat.

Each signal was sampled at 10,000 samples per second (10 kHz), and a total of 900 milliseconds (100 ms pre + 900 ms post) were digitized. This produced digital signals that are 10,000 samples long, a significant burden for most signal processing software. Since relevant pulse events occur early in the blast, the plots and analysis were limited to the first 400 ms of the signals.

In this appendix, all signals are plotted as a set of triaxial signals and their resultant. The following table lists the figures included in this appendix, and indicates with x (forward) , y (lateral), or z (vertical) those signals which appear to be of acceptable quality, and with an asterisk (*) when the signal obviously is unusable because of suspected hardware failures.

Page: Figure	Signals	Triaxial transducer	Suspected problem
29: A-1	* Y Z	Truck cab accelerations	Slow drift after impact.
30: A-2	* * *	Truck bumper accelerations	Broken cables?
31: A-3	X Y Z	Seat accelerations, passenger	None.
32: A-4	* * *	Head accelerations, driver	Bottom out, open cable.
33: A-5	X Y Z	Head accelerations, passenger	None.
34: A-6	X Y Z	Neck forces, driver	None.
35: A-7	X Y Z	Neck forces, passenger	None.
36: A-8	* * *	Chest accelerations, driver	Open ground?
37: A-9	X Y Z	Pelvis accelerations, passenger	None.
38: A-10	X Y Z	Back (lumbar) forces, driver	None.
39: A-11	X Y Z	Back (lumber) forces, passenger	None.

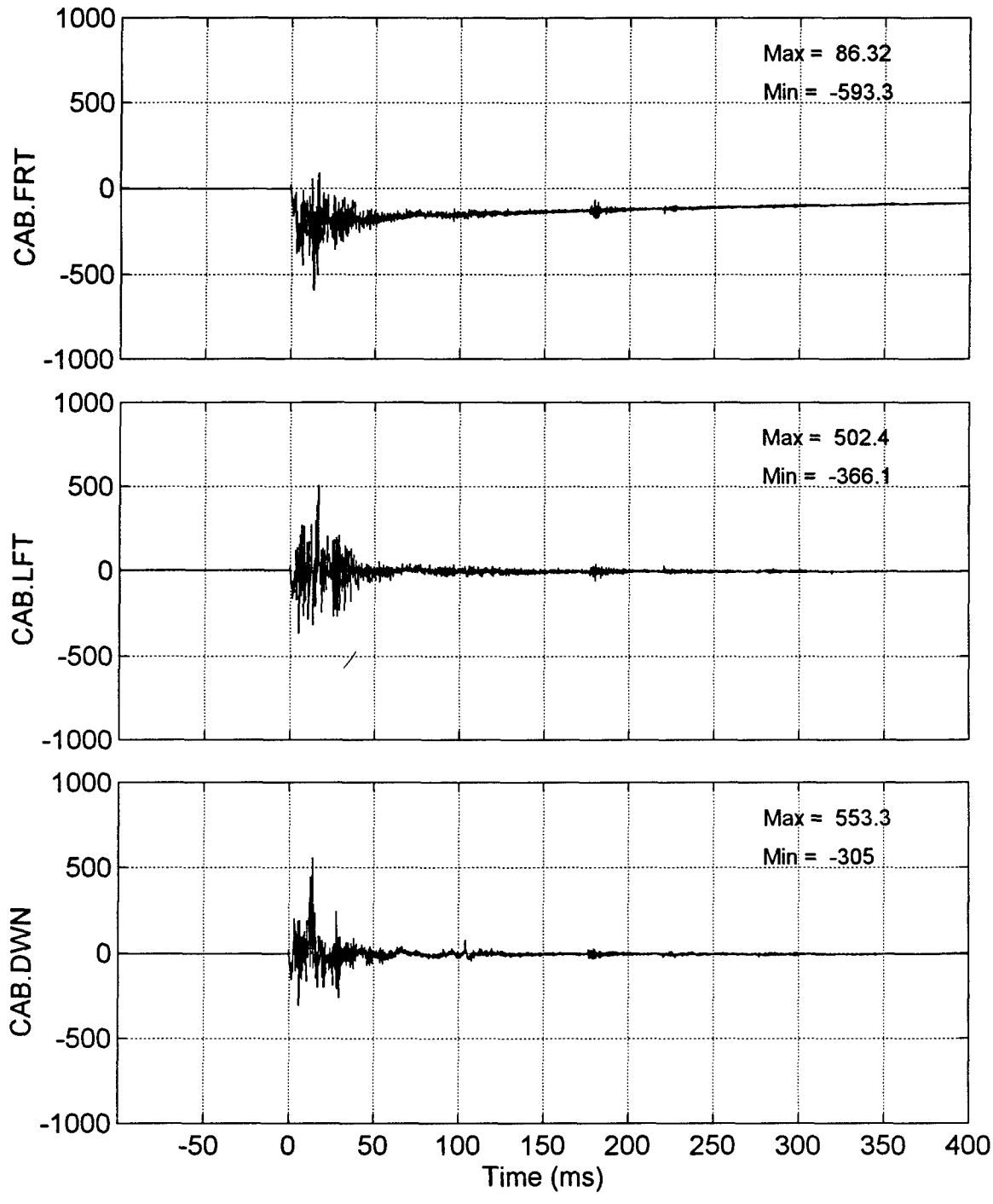

Figure A-1. Truck cab accelerations.

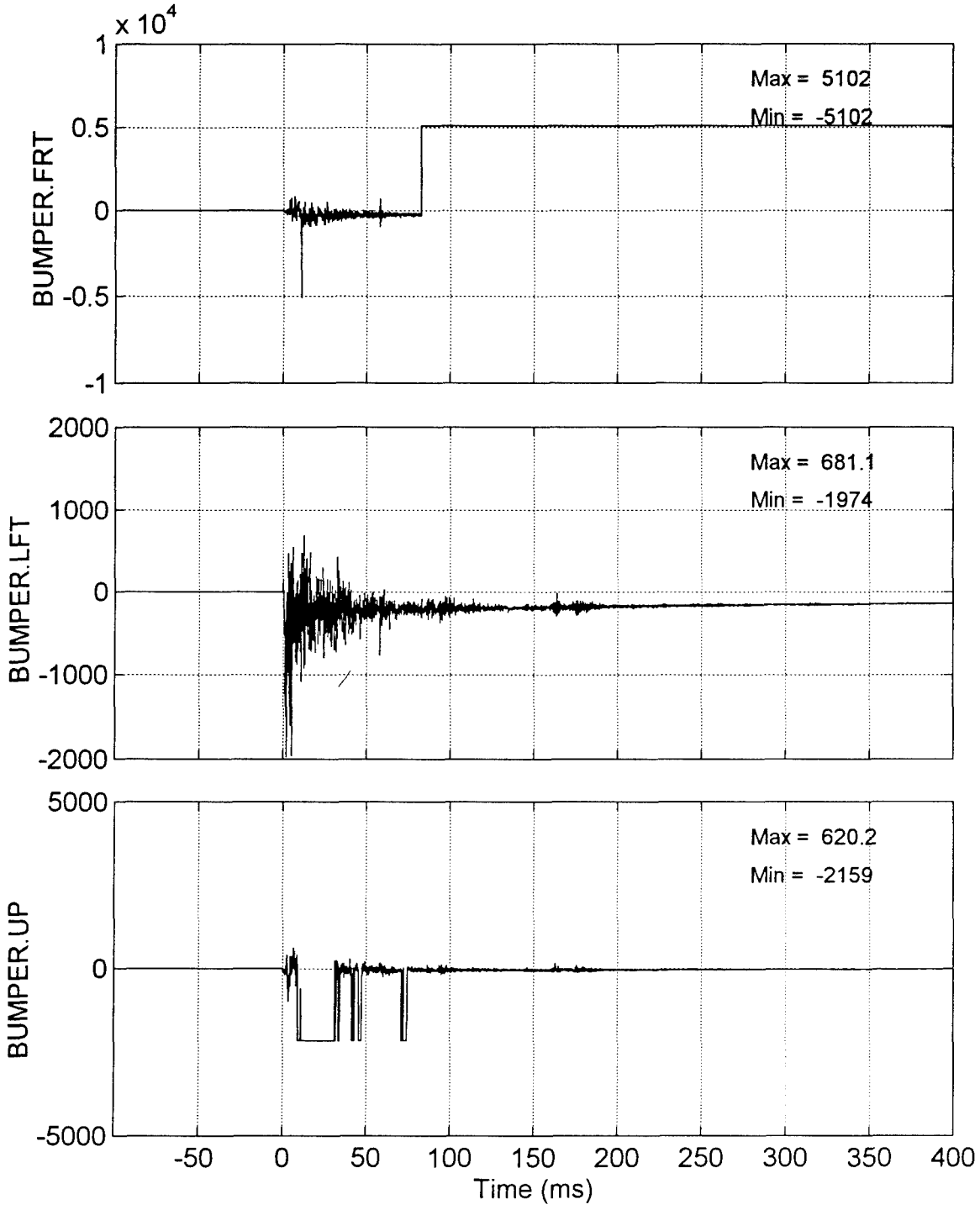

Figure A-2. Truck bumper accelerations.

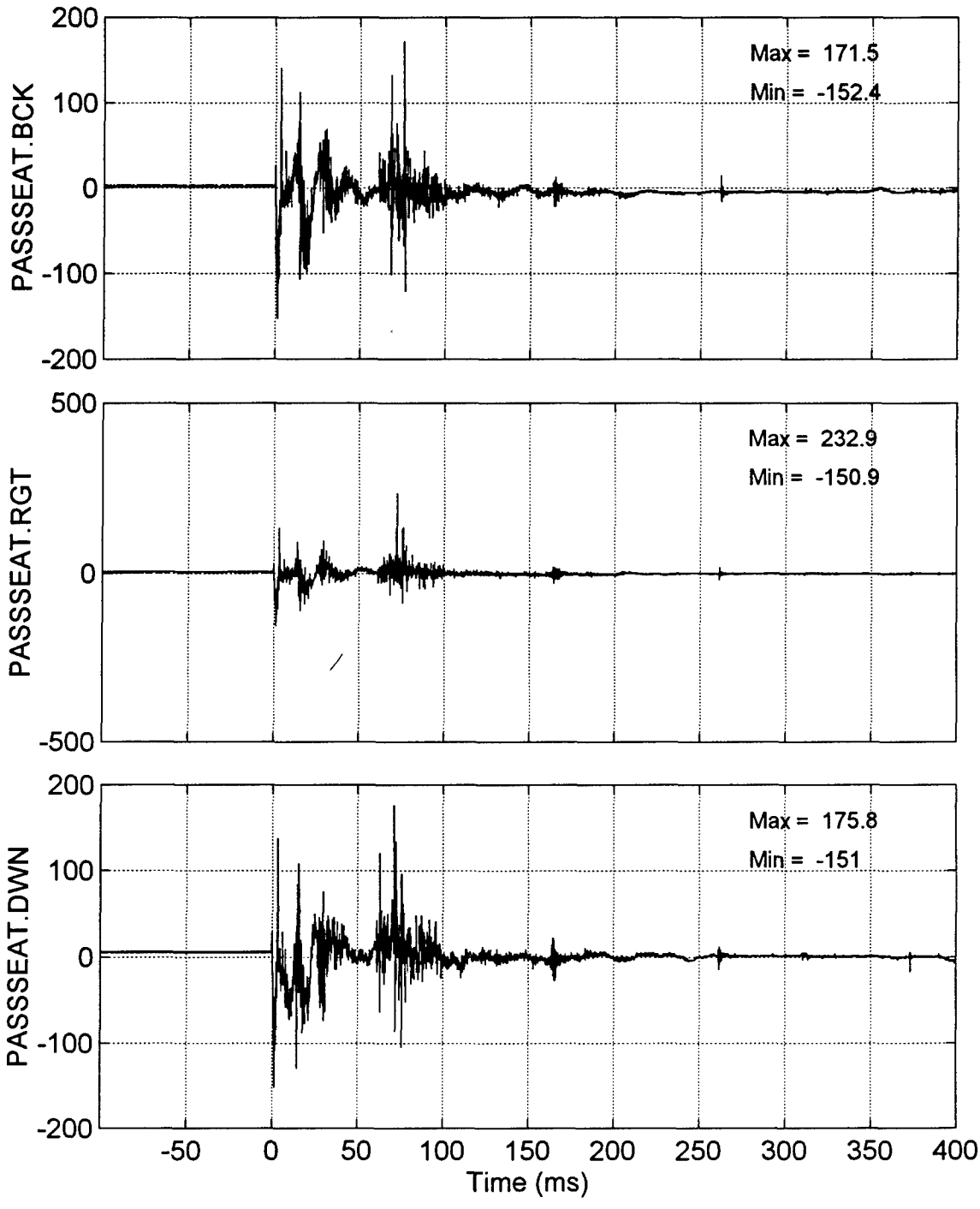

Figure A-3. Seat accelerations, passenger.

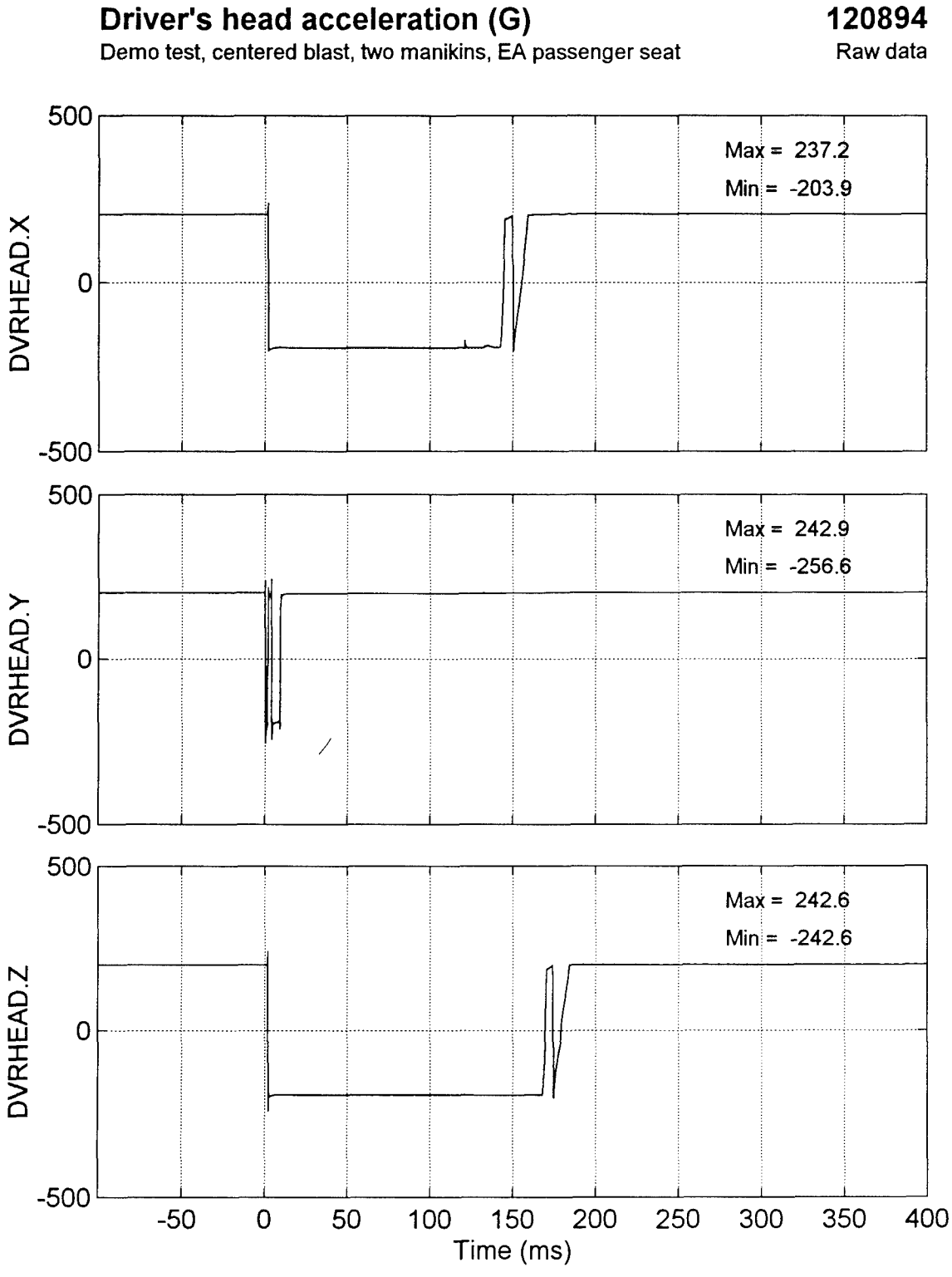

Figure A-4. Head accelerations, driver.

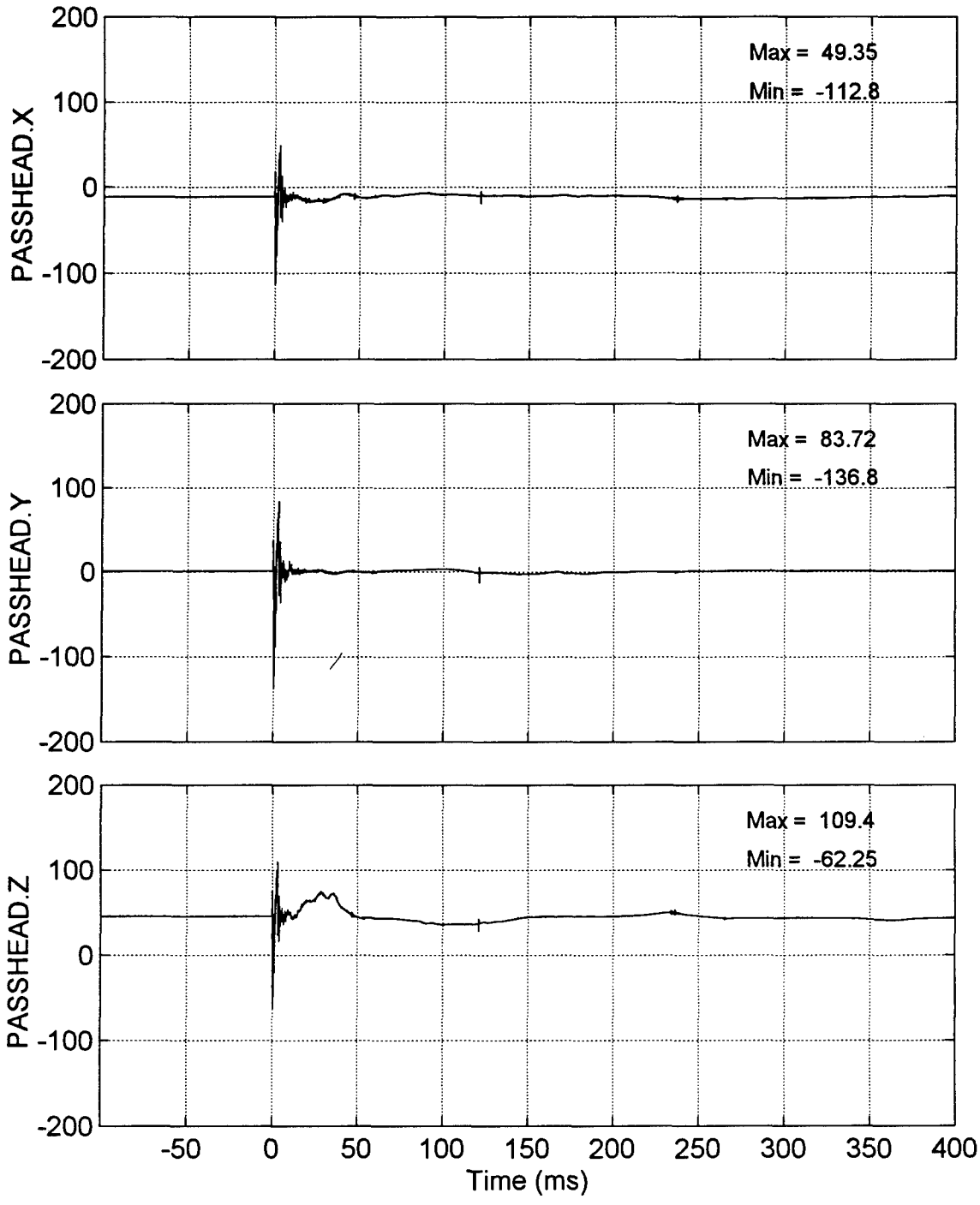

Figure A-5. Head accelerations, passenger.

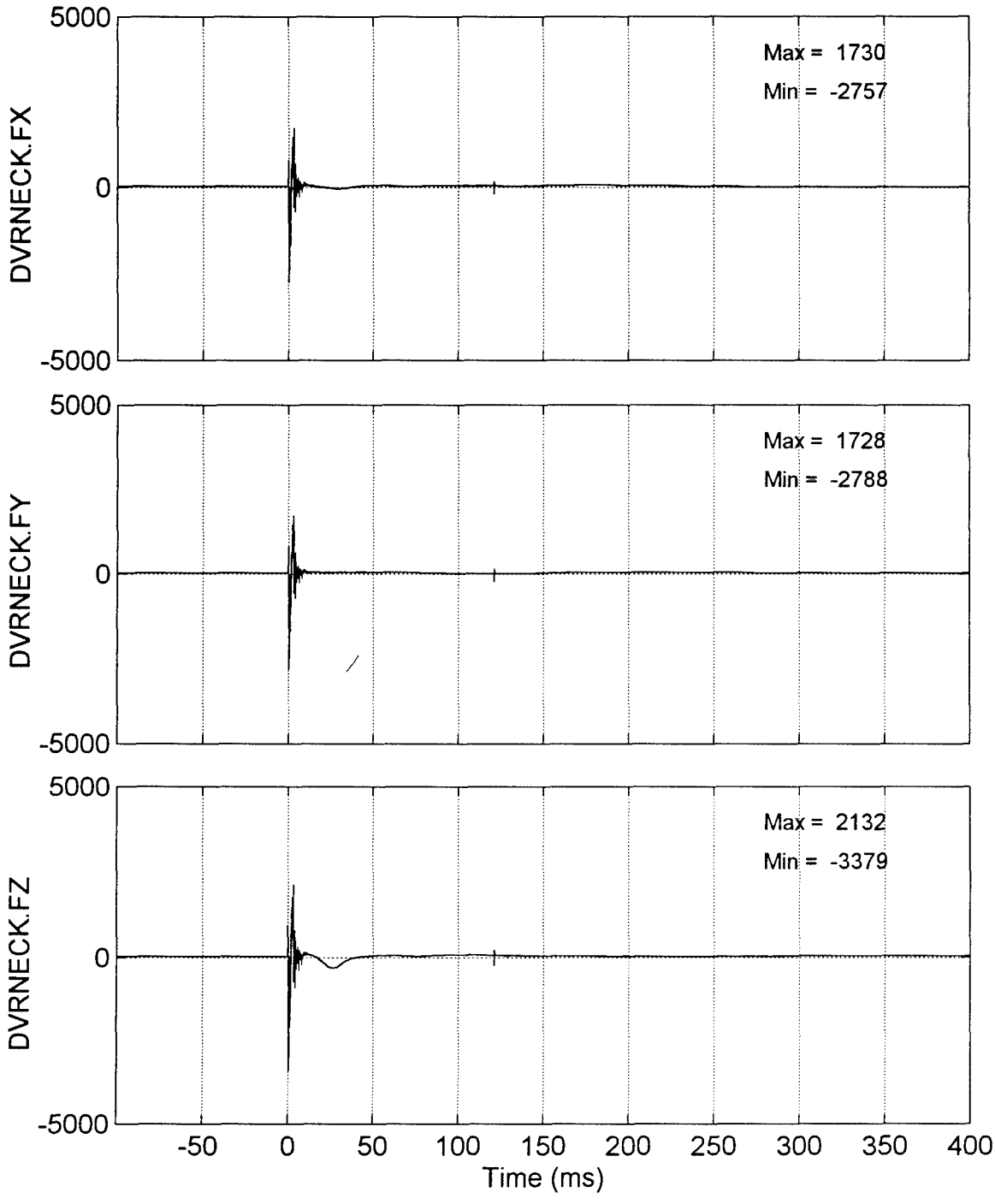

Figure A-6. Neck forces, driver.

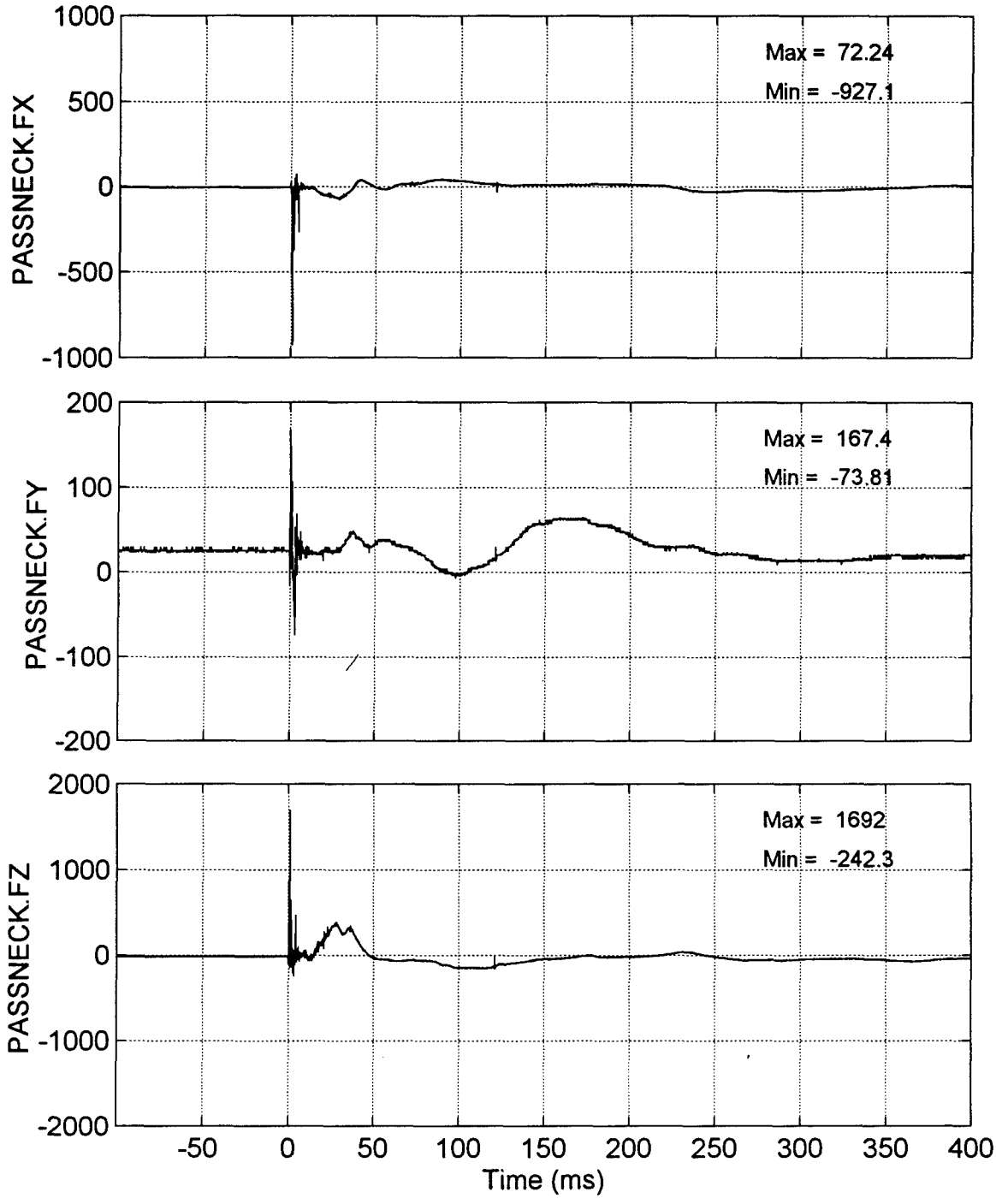

Figure A-7. Neck forces, passenger.

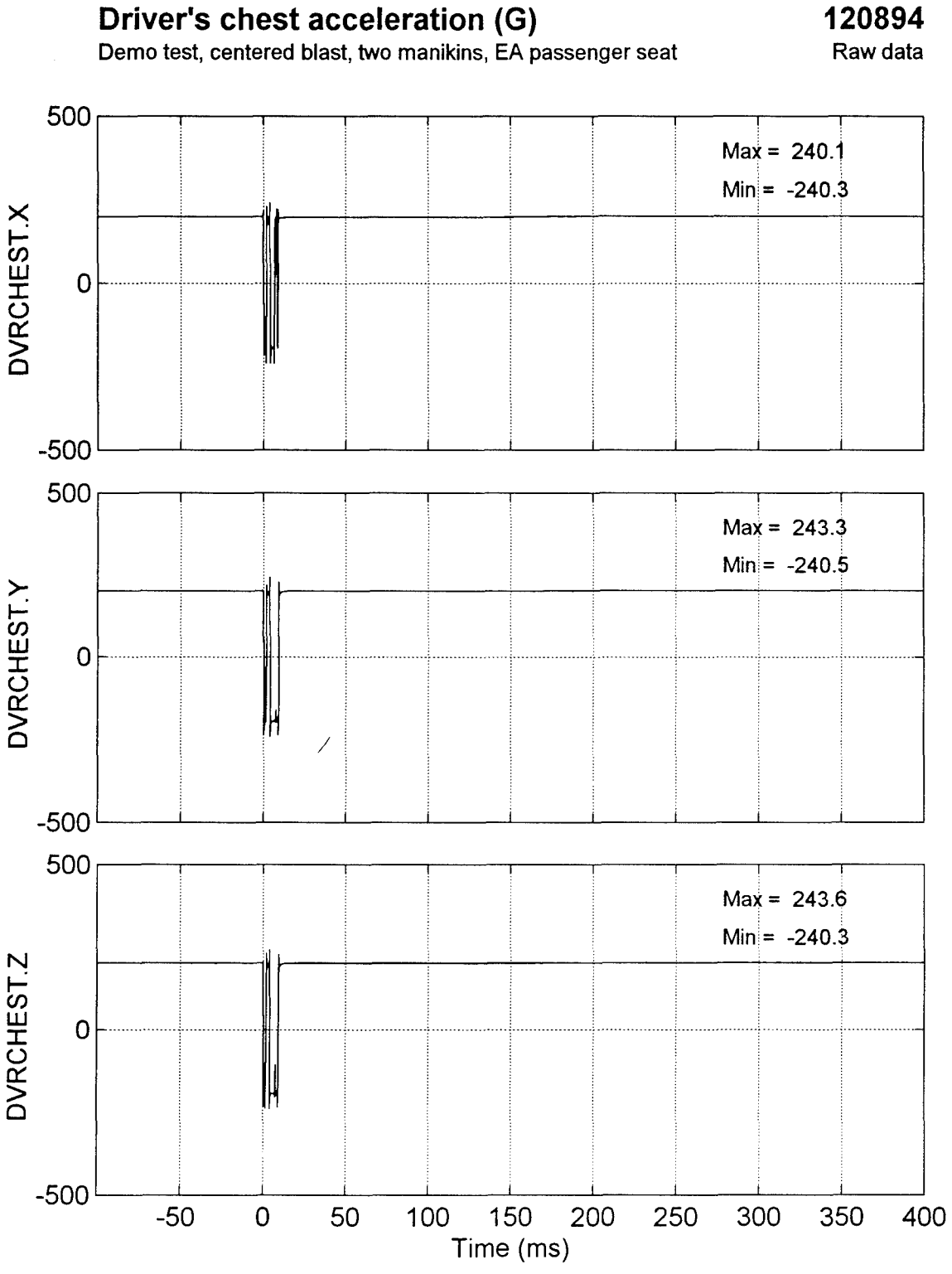

Figure A-8. Chest accelerations, driver.

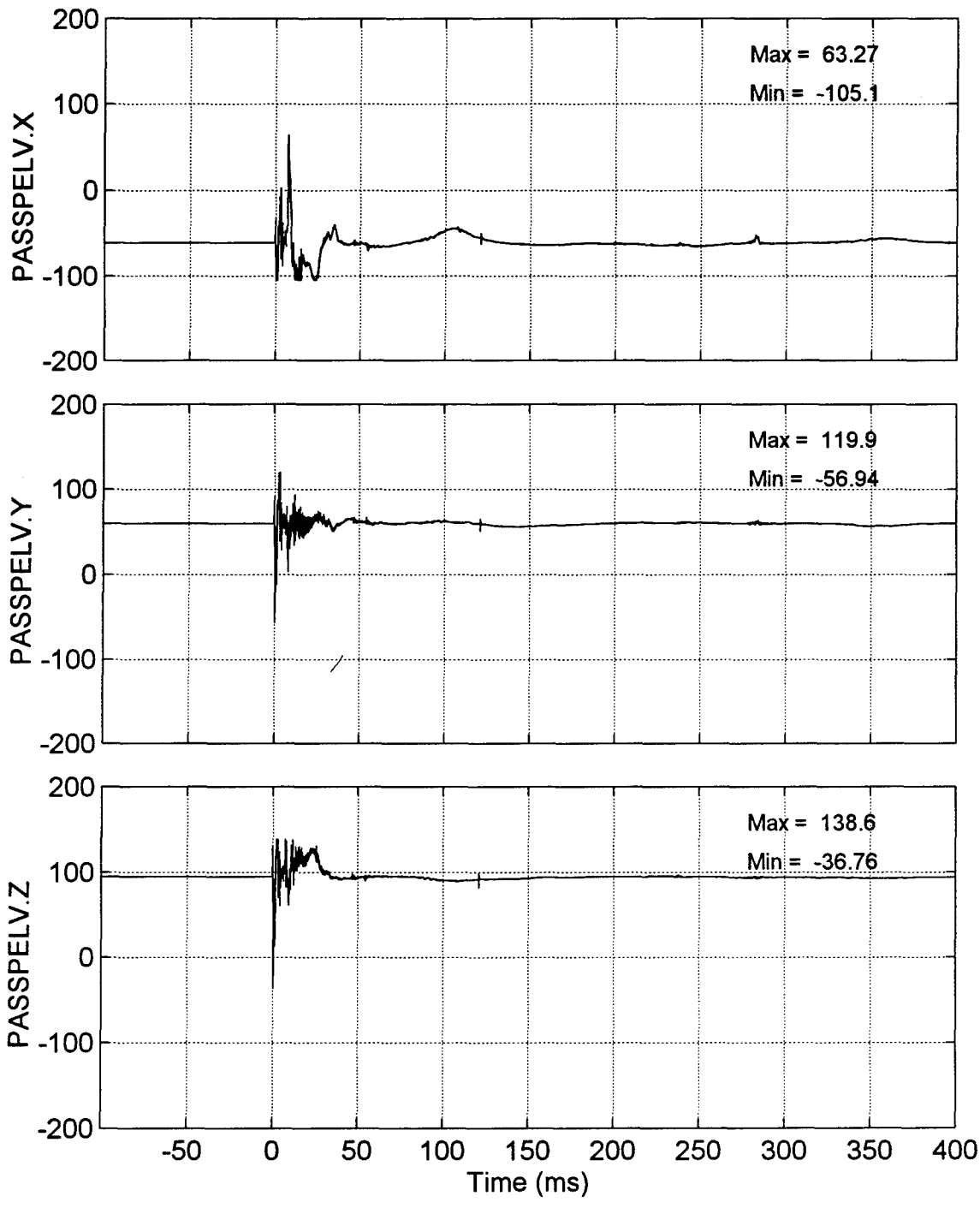

Figure A-9. Pelvis accelerations, passenger.

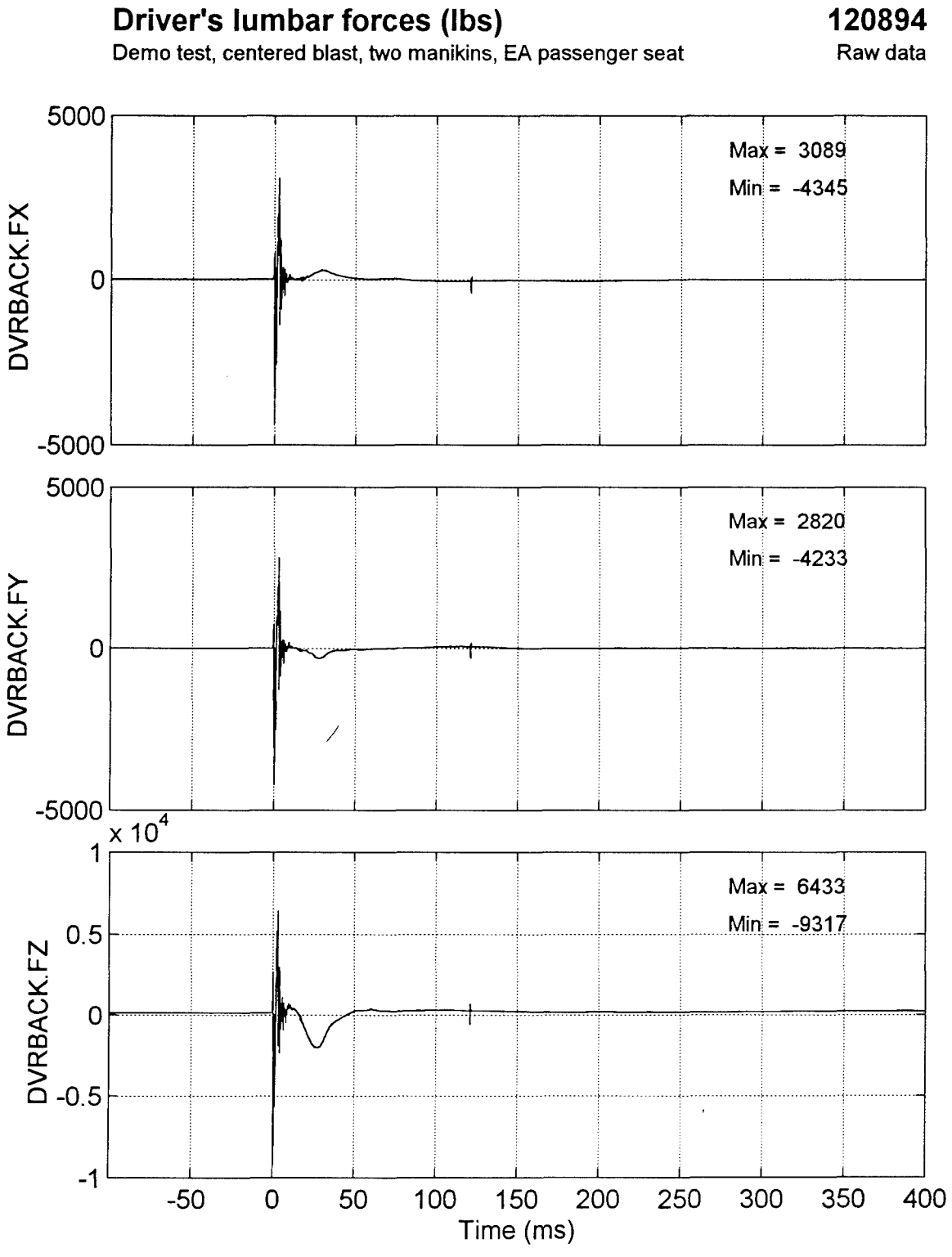

Figure A-10. Back (lumbar) forces, driver.

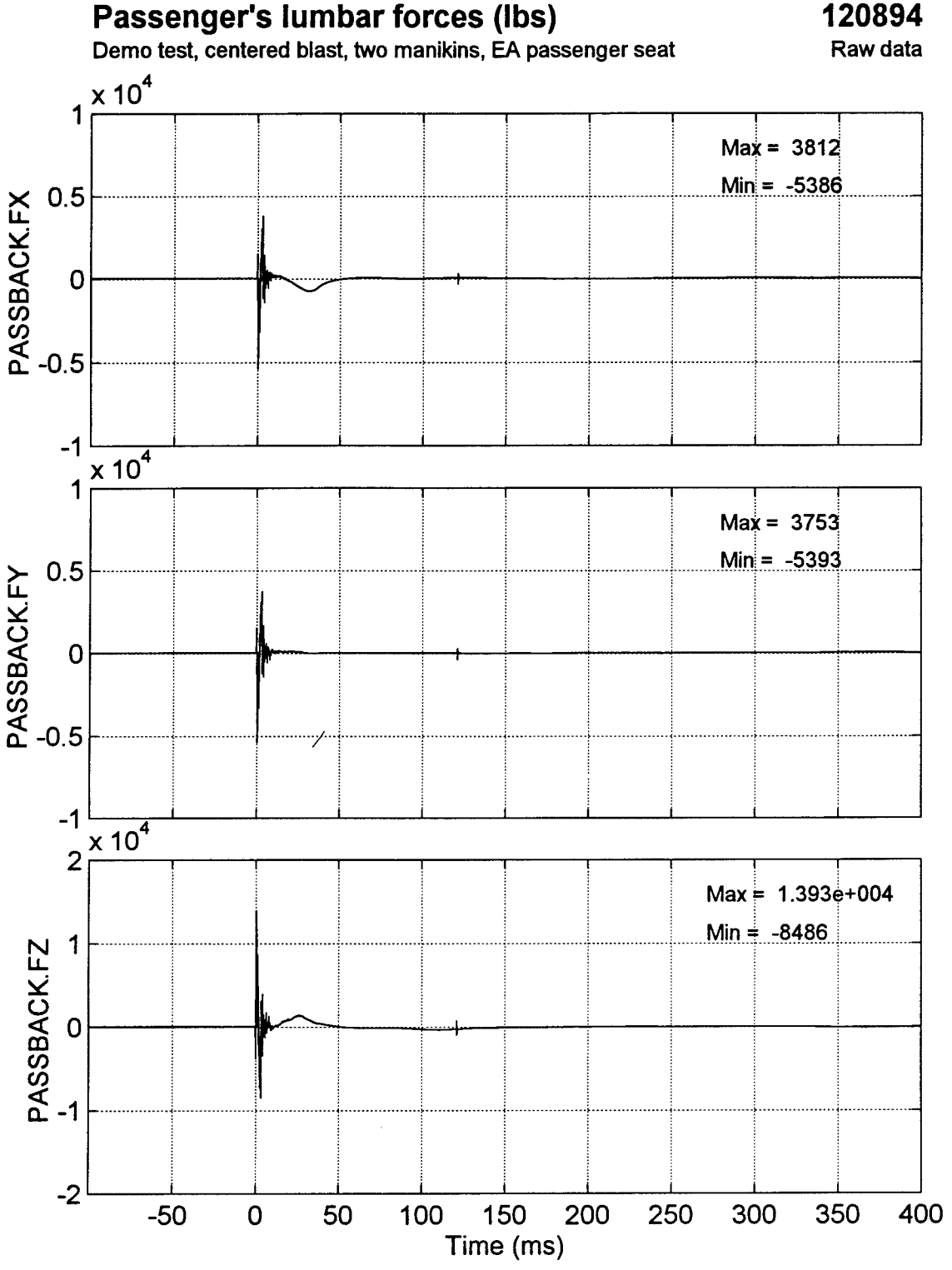

Figure A-11. Back (lumber) forces, passenger.

Appendix B.

Filtered transducer data of test 120894.

This appendix contains the filtered signals of the 11 triaxial transducers used in the mine blast test of 8 December 1994. The filters used are those recommended in the SAE J211 guidelines, as described in the body of the report. Prior to filtering, each signal was zero-adjusted by removing a bias determined from a flat portion after the impact. If necessary, the preimpact segment was set to zero.

The 11 figures of filtered data presented in this appendix correspond to those unfiltered signals given in the 11 figures of Appendix A. The following table lists all 11 figures, including those which were judged of poor quality because of hardware problems (see Appendix A). The reason for this is to demonstrate the pitfall of "automated" signal processing which may produce realistic looking signals, leading to erroneous conclusions.

Page:	Figure	Signals	Triaxial transducer	Filter 3-dB corner
41:	B-1	* Y Z	Truck cab accelerations	100 Hz
42:	B-2	* * *	Truck bumper accelerations	100 Hz
43:	B-3	X Y Z	Seat accelerations, passenger	100 Hz
44:	B-4	* * *	Head accelerations, driver	1000 Hz
45:	B-5	X Y Z	Head accelerations, passenger	1000 Hz
46:	B-6	X Y Z	Neck forces, driver	300 Hz
47:	B-7	X Y Z	Neck forces, passenger	300 Hz
48:	B-8	* * *	Chest accelerations, driver	300 Hz
49:	B-9	X Y Z	Pelvis accelerations, passenger	300 Hz
50:	B-10	X Y Z	Back (lumbar) forces, driver	300 Hz
51:	B-11	X Y Z	Back (lumber) forces, passenger	300 Hz

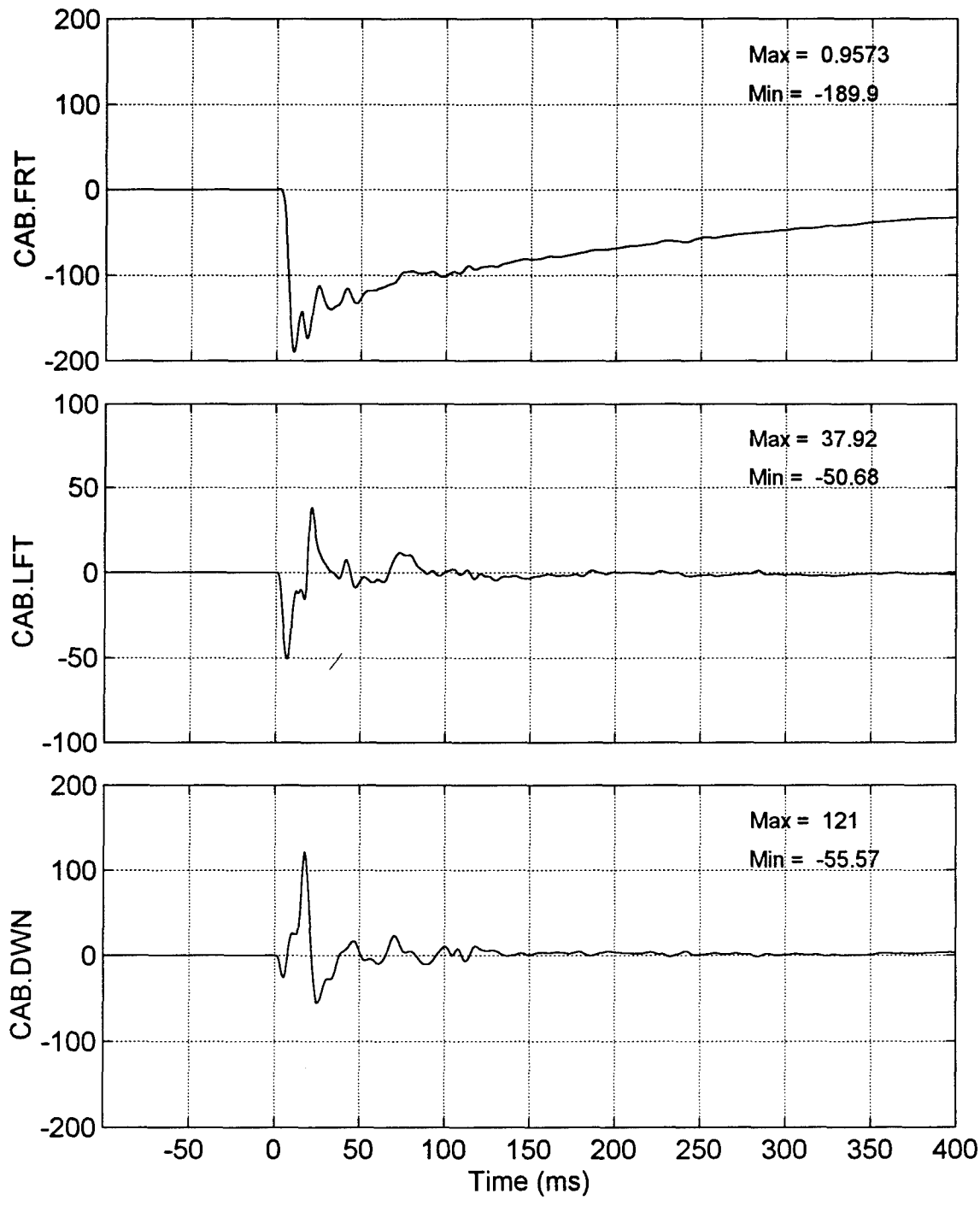

Figure B-1. Filtered truck cab accelerations.

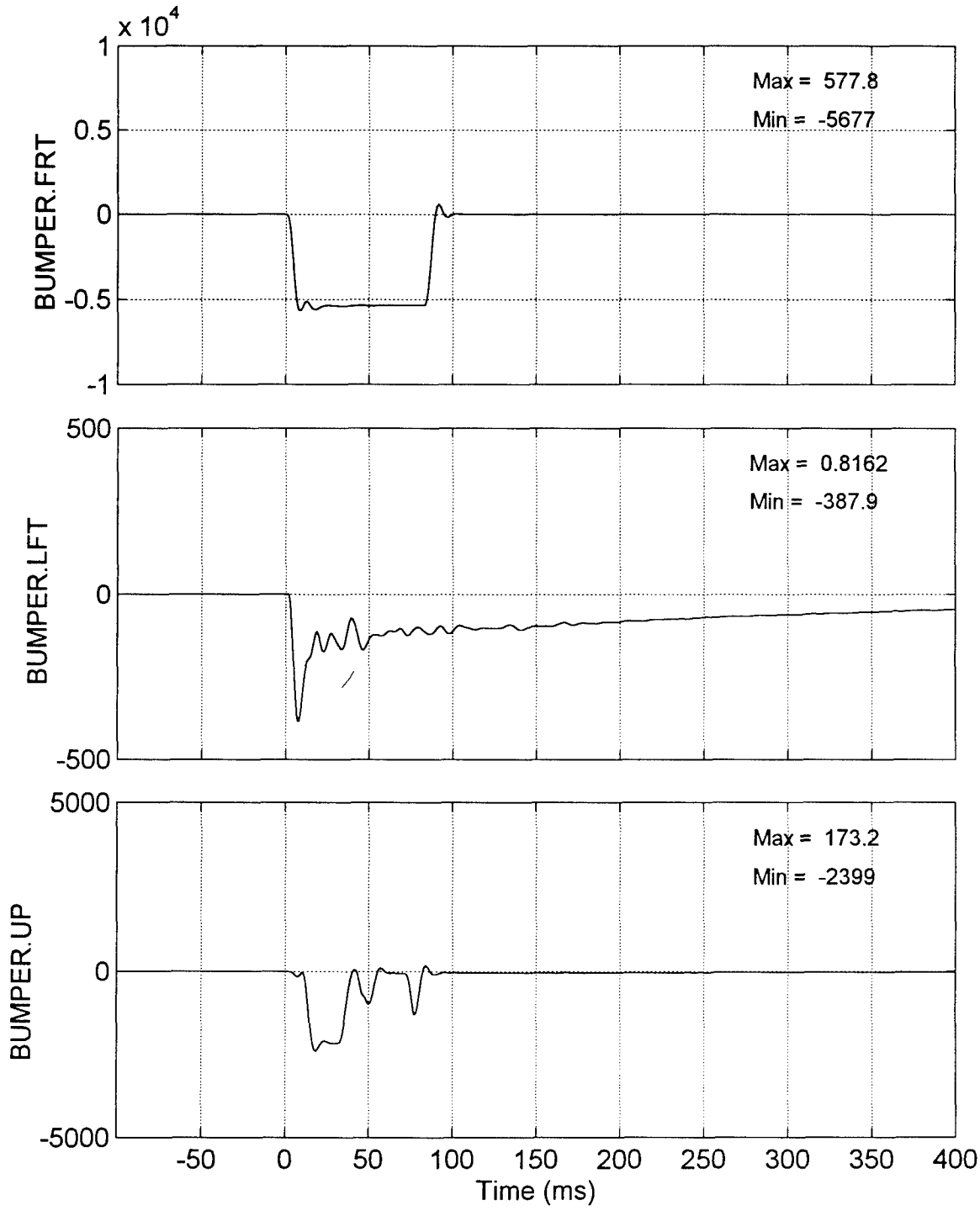

Figure B-2. Filtered truck bumper accelerations.

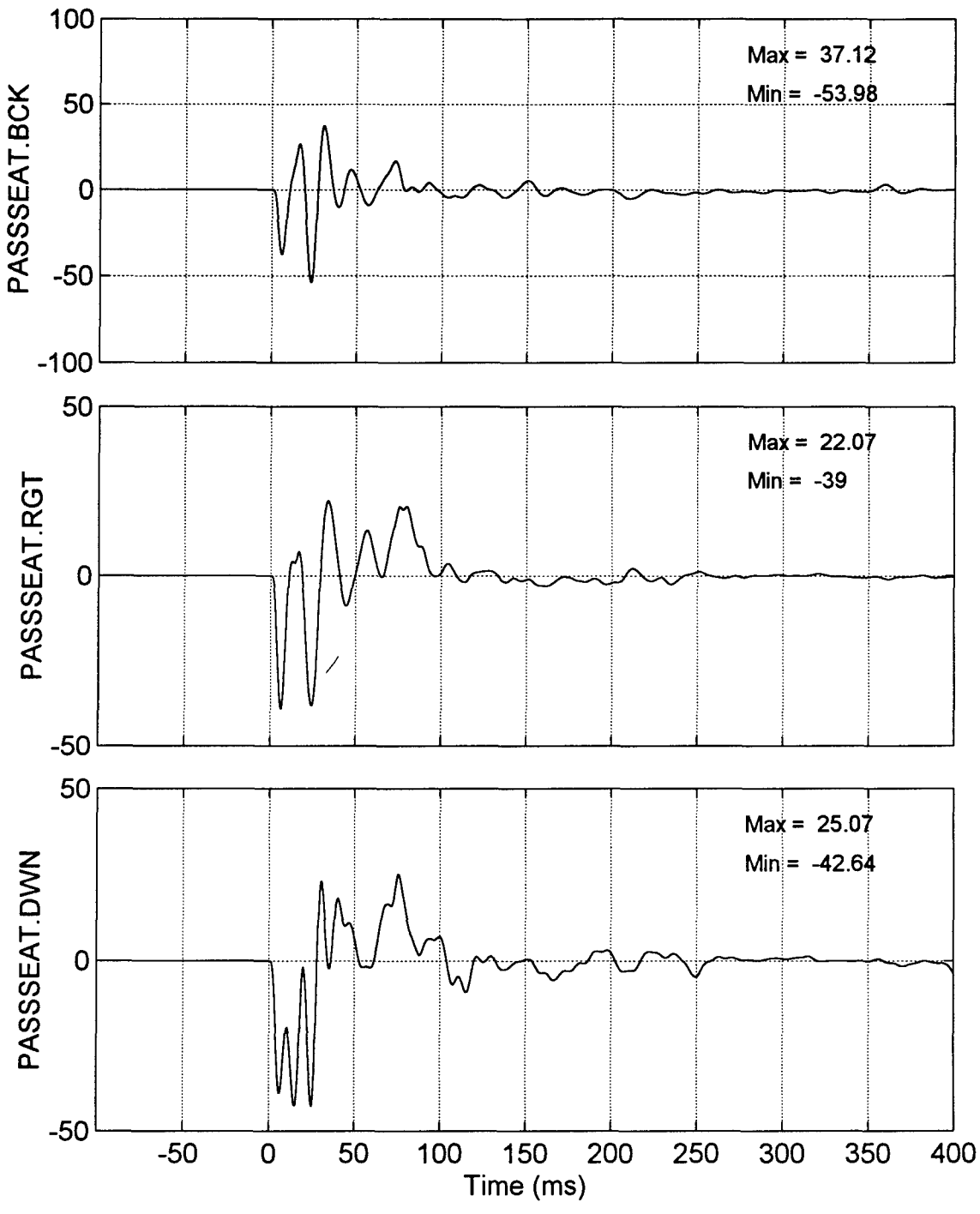

Figure B-3. Filtered seat accelerations, passenger.

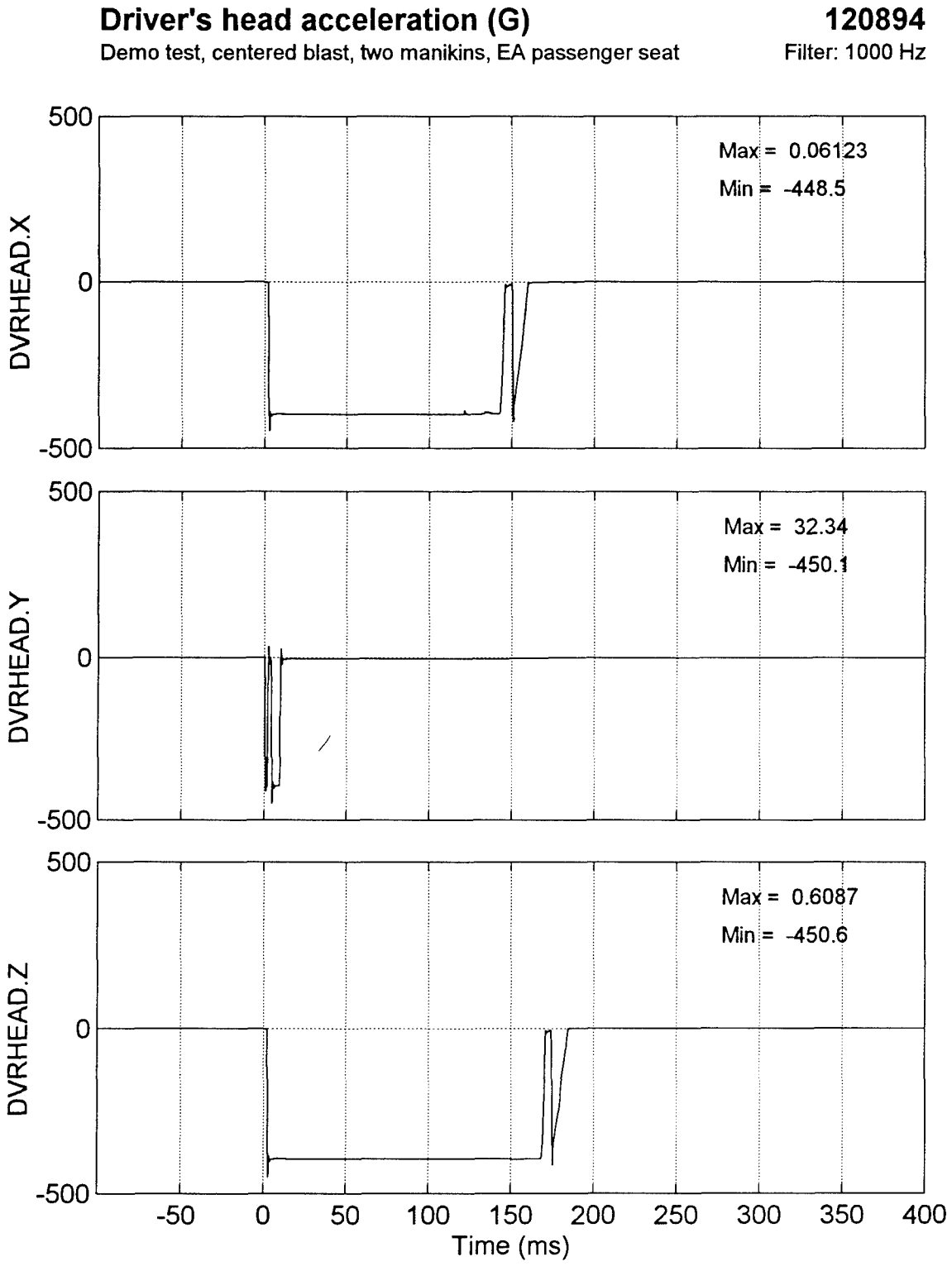

Figure B-4. Filtered head accelerations, driver.

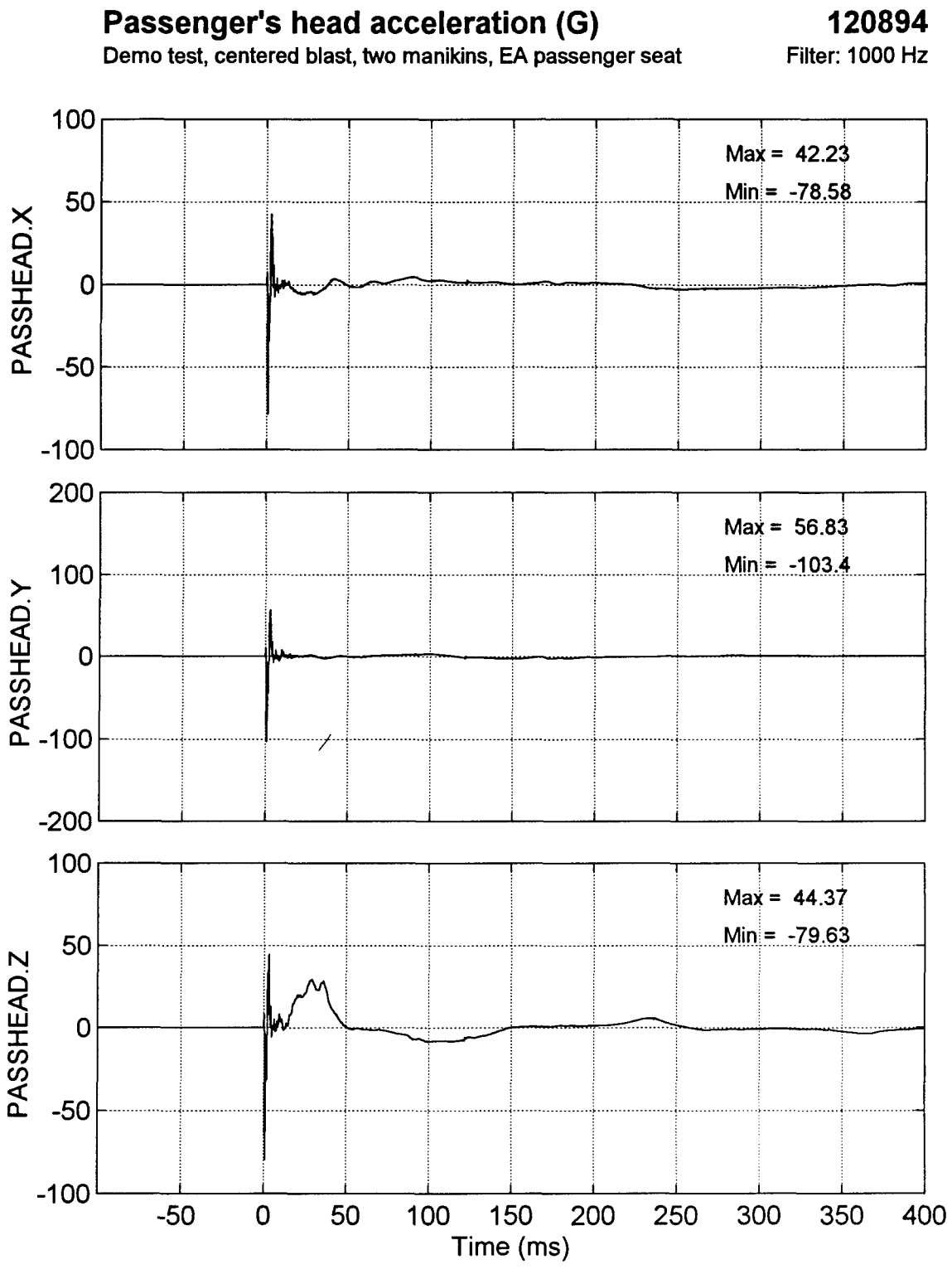

Figure B-5. Filtered head accelerations, passenger.

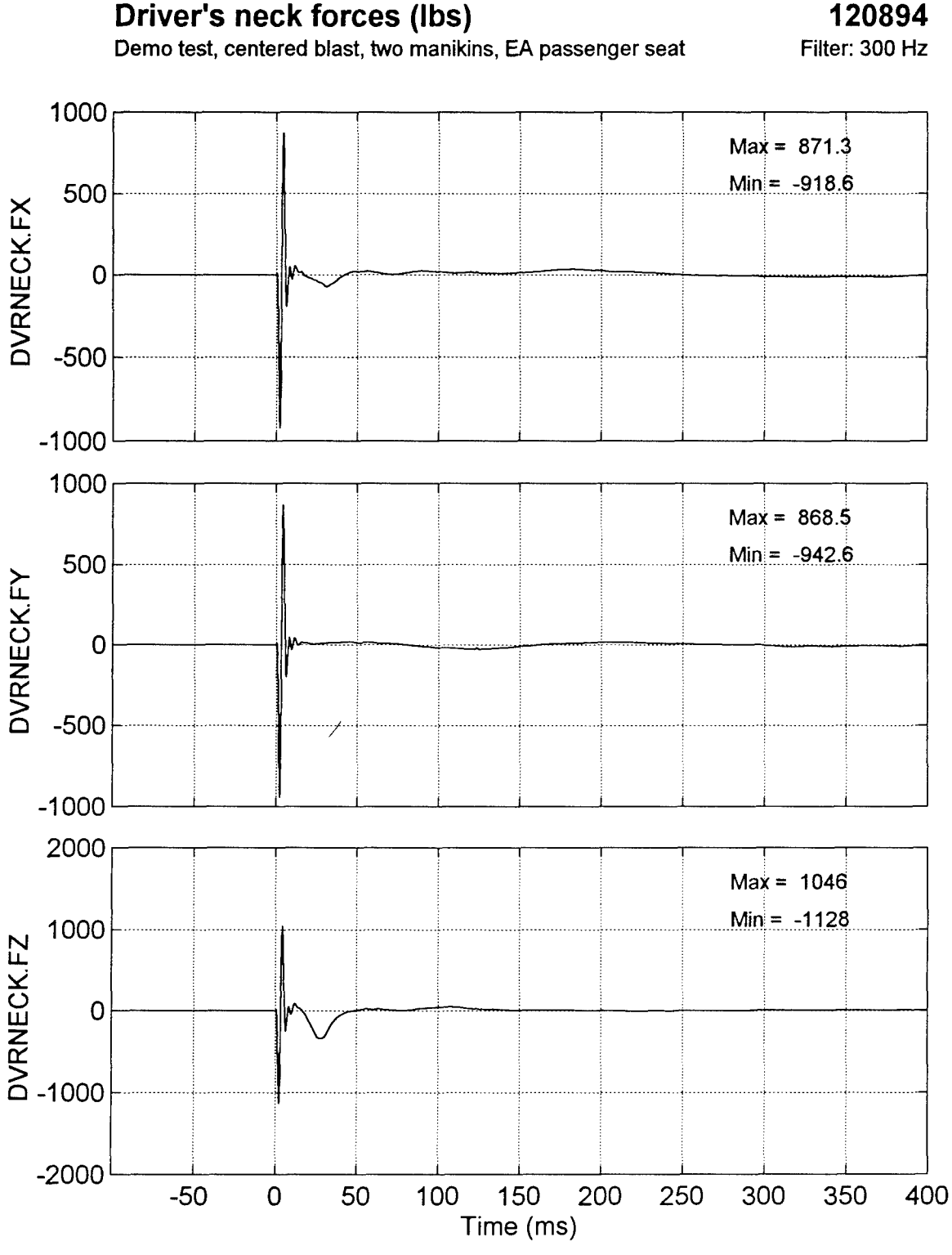

Figure B-6. Filtered neck forces, driver.

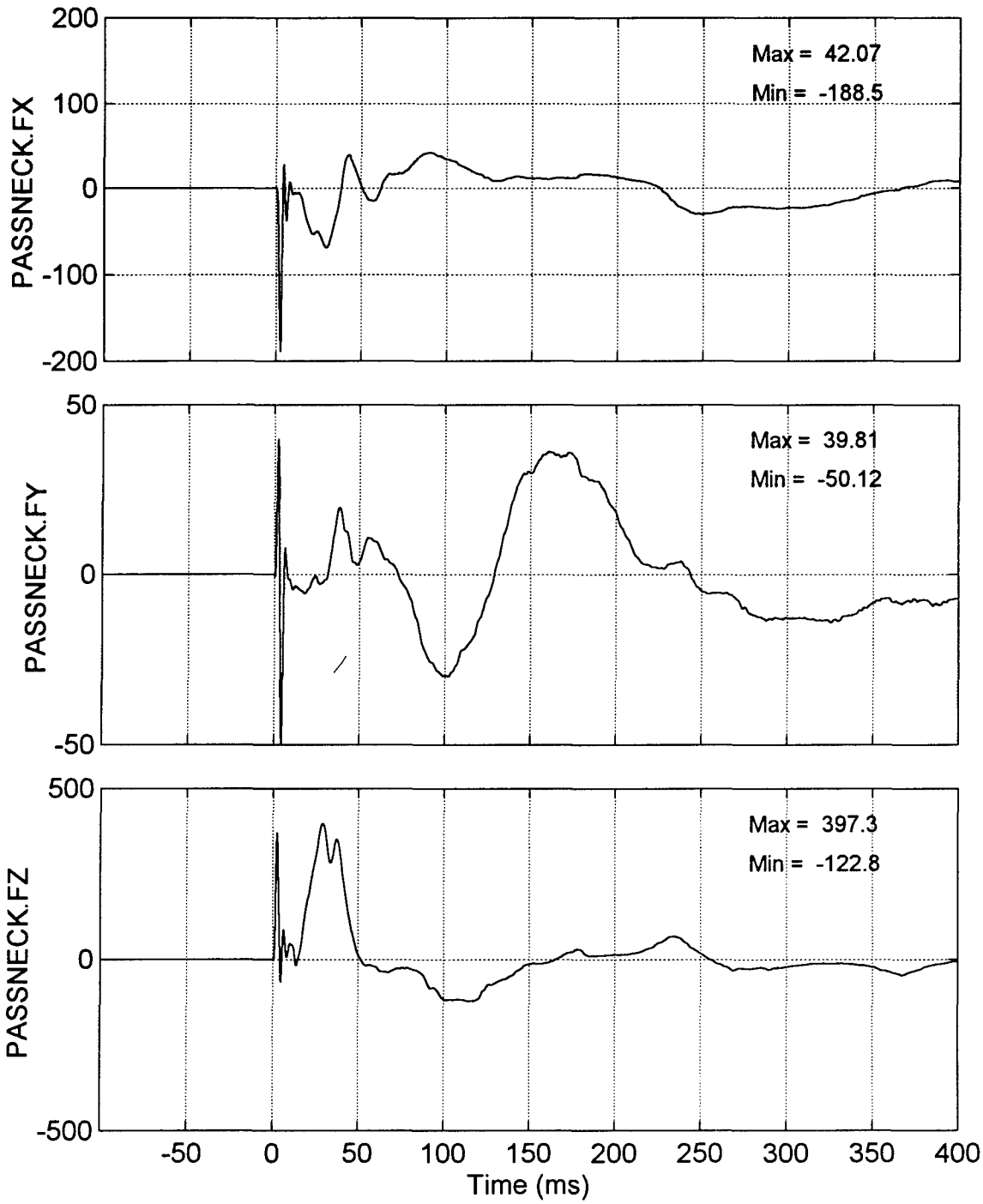

Figure B-7. Filtered neck forces, passenger.

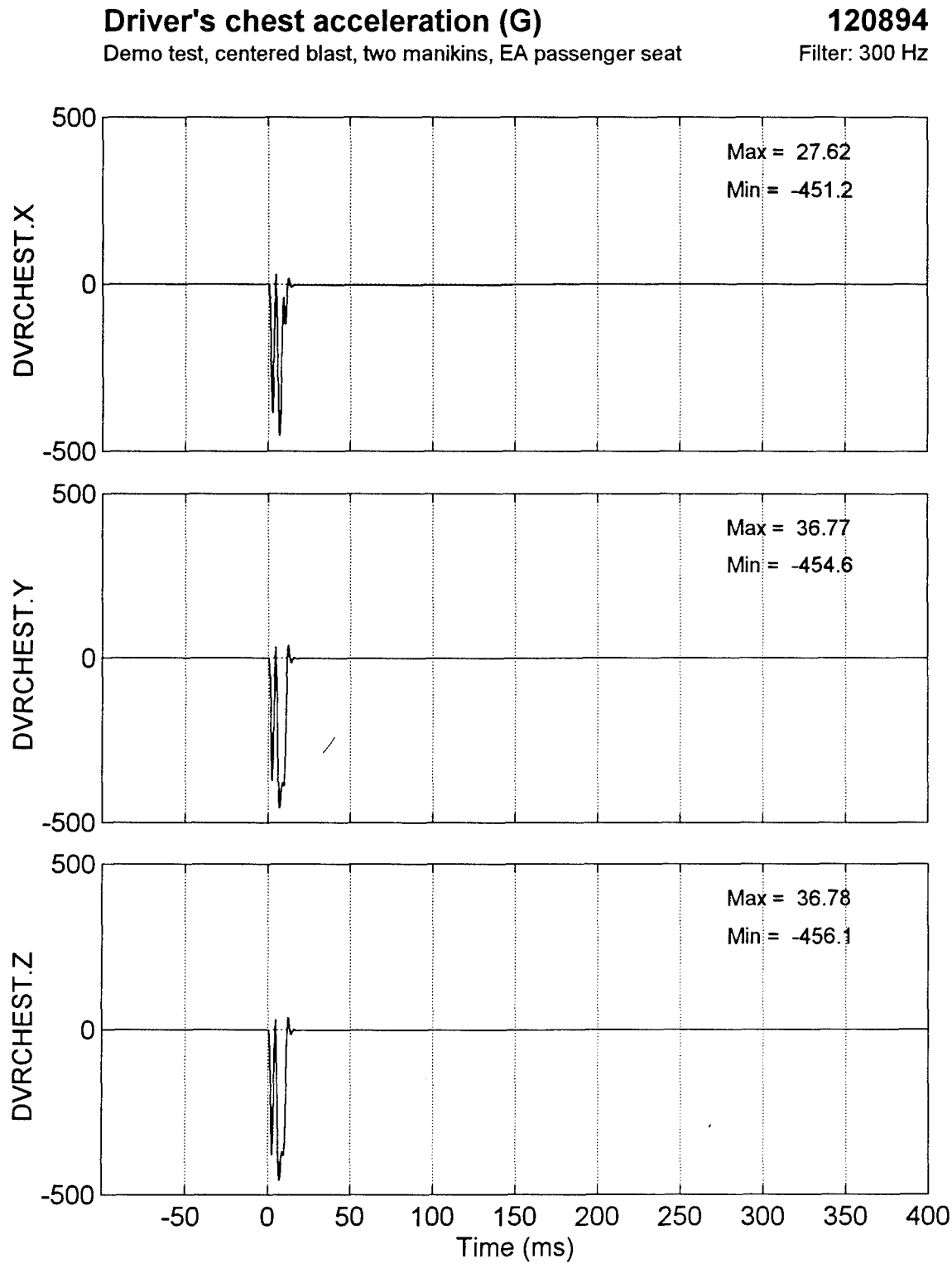

Figure B-8. Filtered chest accelerations, driver.

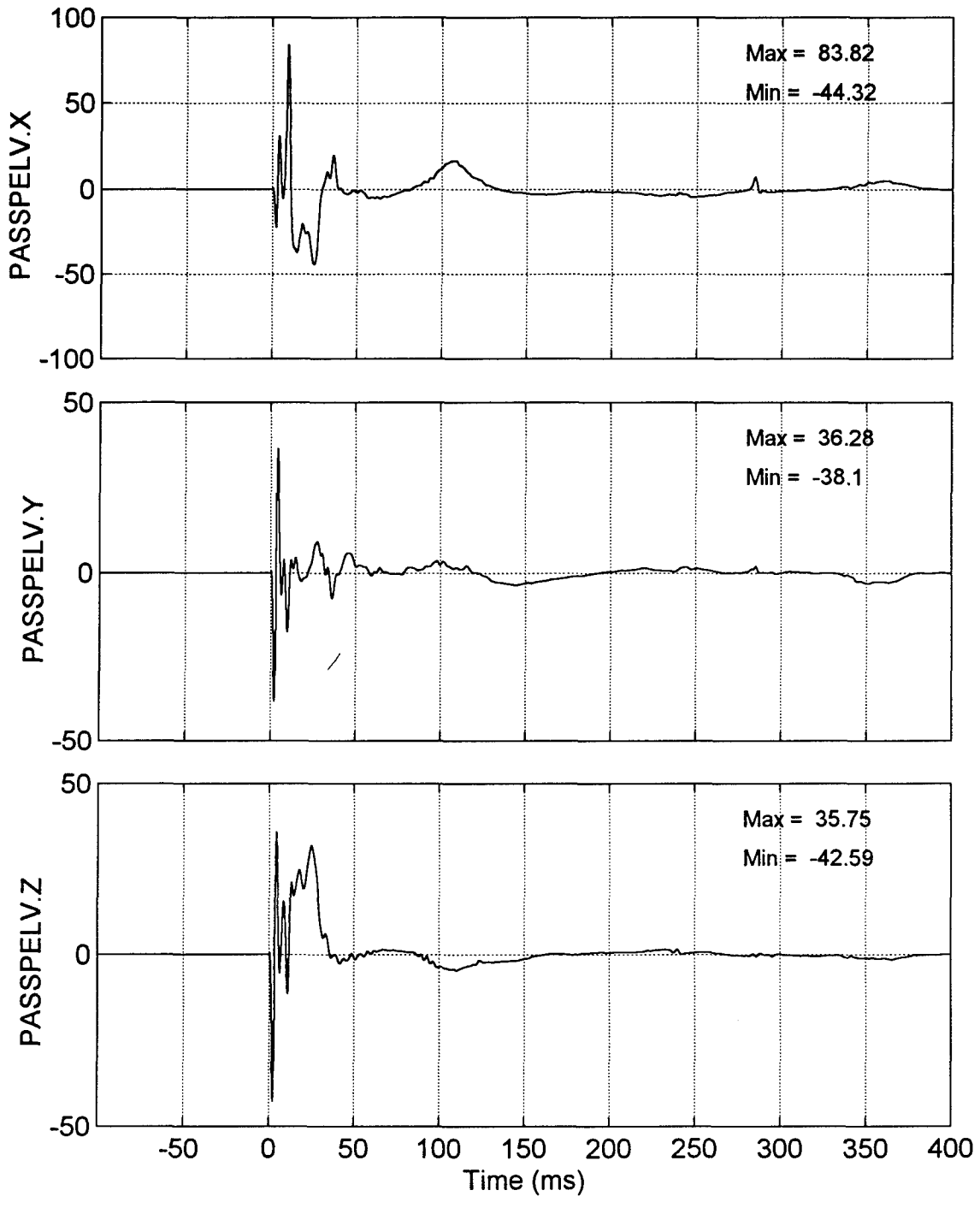

Figure B-9. Filtered pelvis accelerations, passenger.

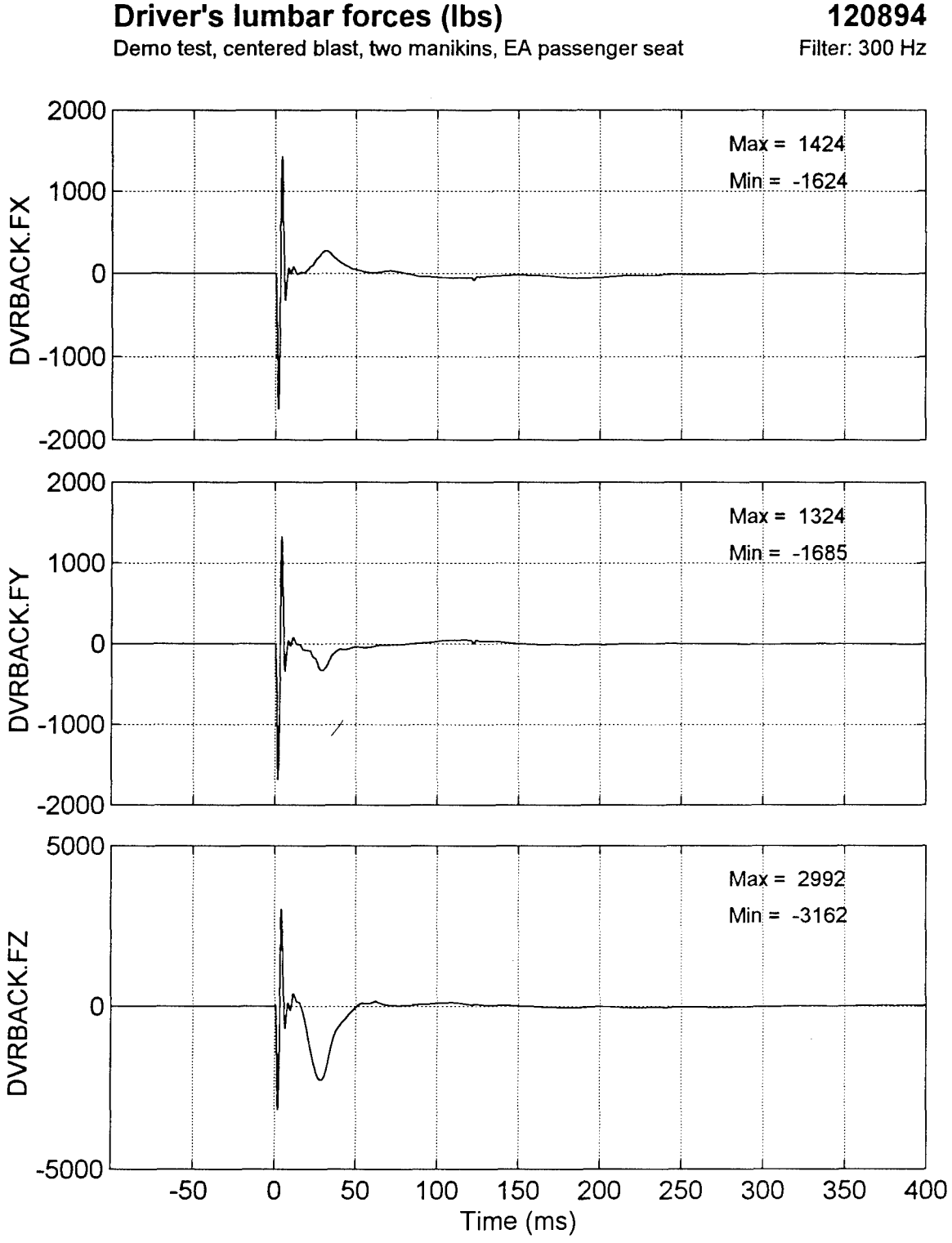

Figure B-10. Filtered back (lumbar) forces, driver.

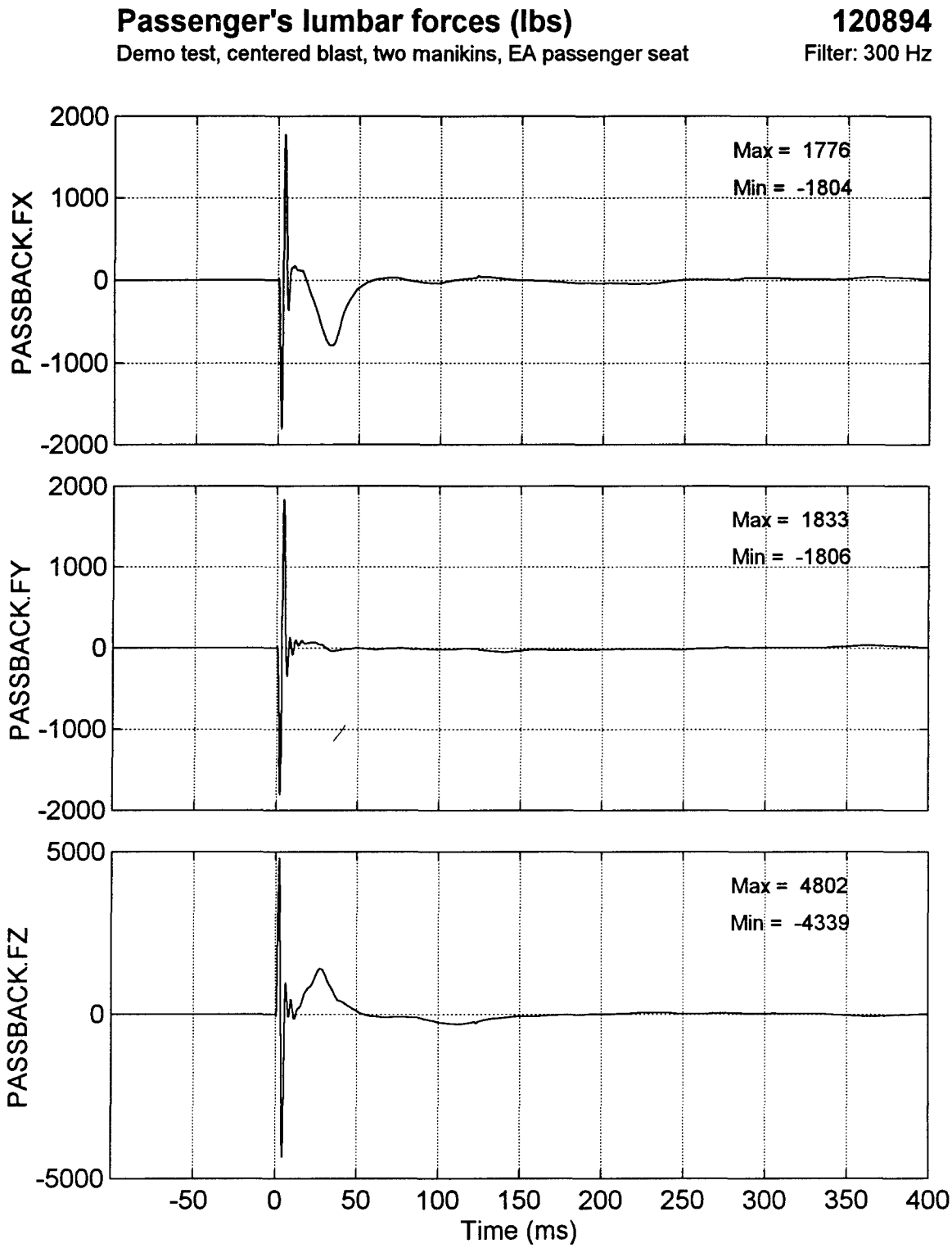

Figure B-11. Filtered back (lumber) forces, passenger.

Appendix C.

Effects of signal processing.

The vertical acceleration of the passenger seat is taken as an example to demonstrate the effects of signal processing on the interpretation of results, and to establish an appropriate procedure for manipulating and processing acceleration signals.

In Figure C-1, the upper curve is the raw acceleration signal, plotted in its entirety without filtering and without removing the DC bias. The lower curve is the velocity in the vertical direction, obtained by direct integration of the raw acceleration curve. Clearly, the negative DC bias, visible as a horizontal segment from -10 to 0 msec, causes the velocity to decrease constantly before the impact, an erroneous result.

Assuming that the acceleration is zero before the impact, the DC bias in the (-10,0) segment was subtracted from the entire signal. The result is shown in Figure C-2. Now, the preimpact velocity is correctly shown as zero; however, the velocity continues to increase constantly after the impact event. This indicates that another bias remained in the transducer signal after the impact and did not return to its preimpact DC level of zero.

To remedy the postimpact transducer bias, the true "zero" state of the signal is taken very late after most signal activities have died down. Using an average value of the segment from 45 to 85 msec postimpact as the "zero" of the signal, the acceleration signal was shifted by this constant zero value to produce the results shown in Figure C-3. Since the postimpact "zero" is different from the preimpact "zero," the preimpact velocity was expected to be increasing constantly, as it did in Figure C-3.

Ideally, the transducer and signal conditioning hardware would produce true zero readings before the impact and return to the same zero state after the impact. Fortunately, integration and analysis should start at zero and do not have to include preimpact data. However, preimpact segment provides continuity and perspective on the initiation of the impact and may be assumed to be zero anyway. With this assumption, the integrated velocity curve exhibits all the correct behaviors consistent with the observed truck motion. This is shown in Figure C-4. Note that the peak velocity of the truck seat is 0.8 in/sec, approximately, and the acceleration spikes reach as high as 150 G.

The final step in signal processing of truck and manikin signals is filtering. In our example, we applied the recommended filter of 100 Hz (SAE channel class 60) to the acceleration signal which had been zero-adjusted as described above. This brought out the true gross motion of the seat as the curves in Figure C-5. Clearly, the peak acceleration of the seat in the vertical direction was only 12-13 G and not the 100 G which had been used in some of the simulations.

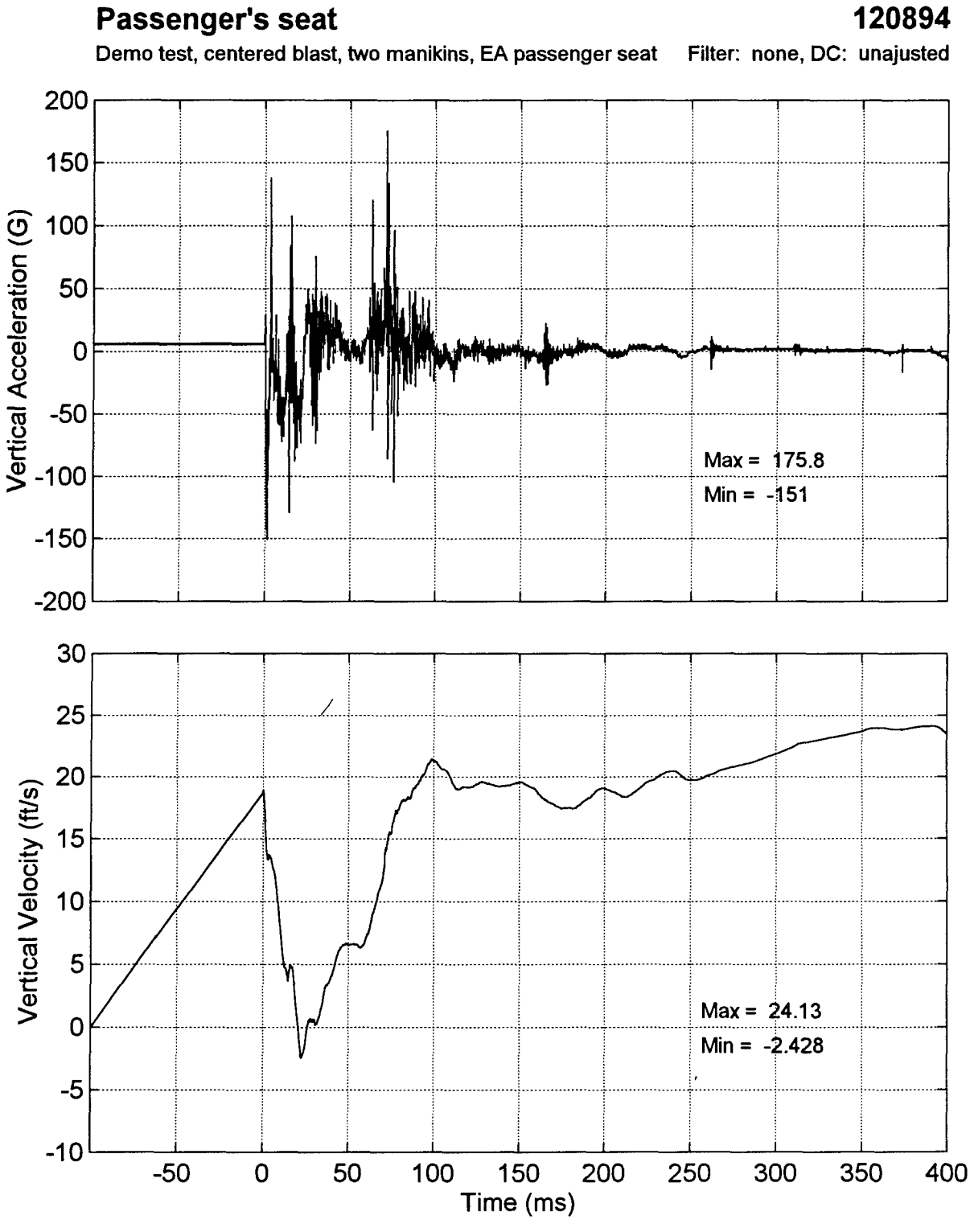

Figure C-1. Effect of zero bias of unfiltered acceleration signal on integrated velocity.

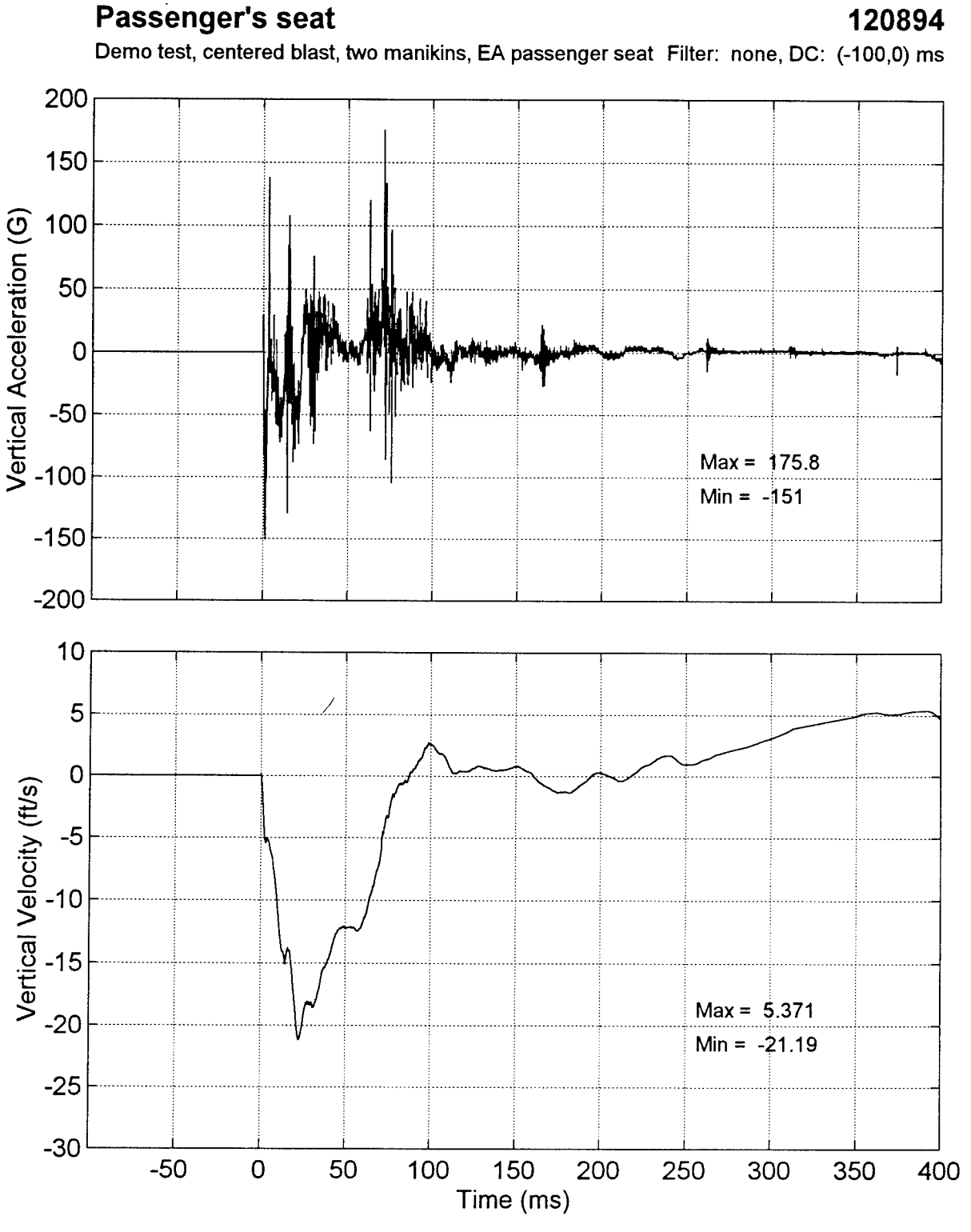

Figure C-2. Velocity obtained by integration of acceleration pulse after removal of zero bias based on 100 ms pre-trigger segment.

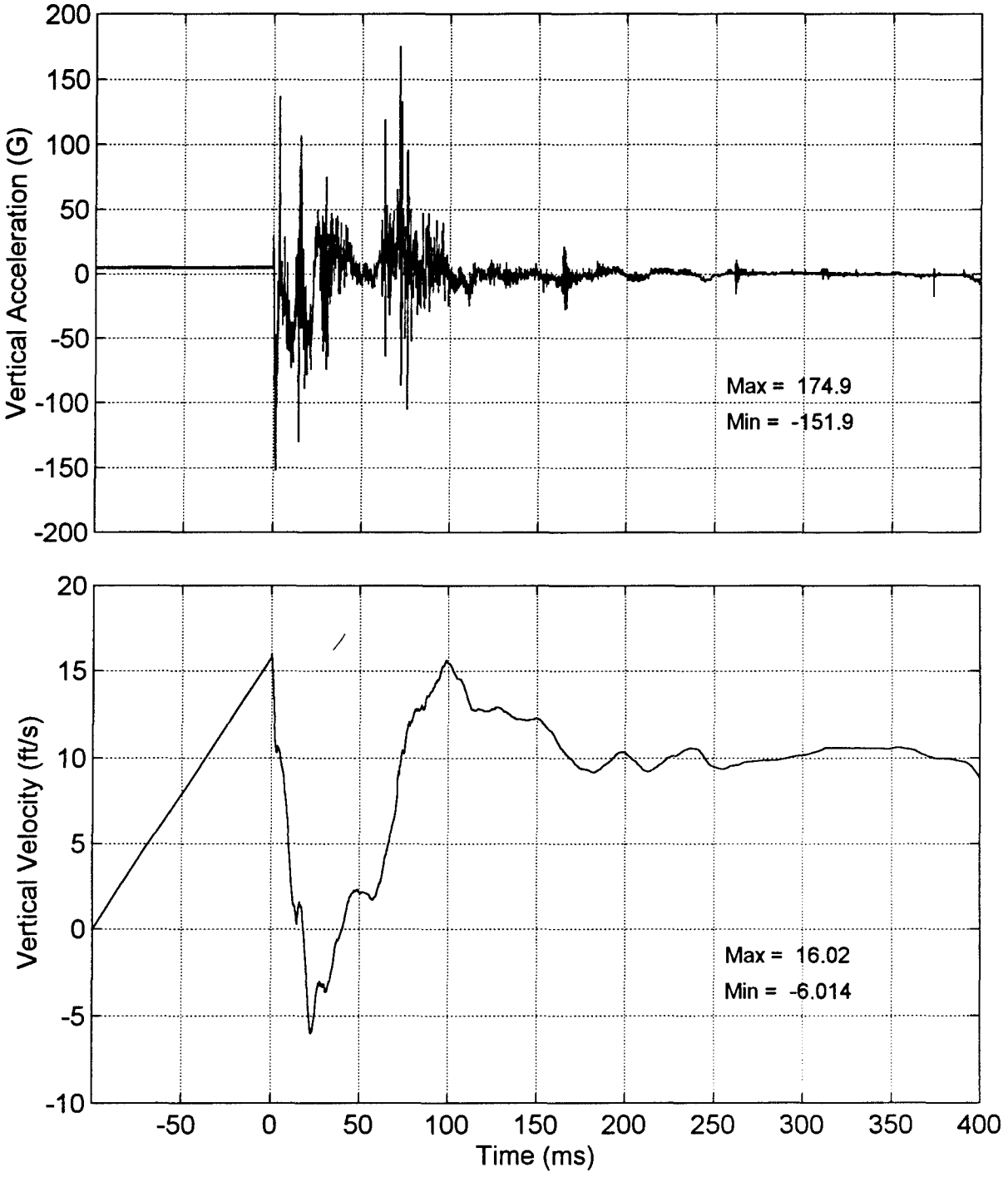

Figure C-3. Acceleration and integrated velocity, assuming that zero level is at end of signal, and without modifying pre-trigger segment.

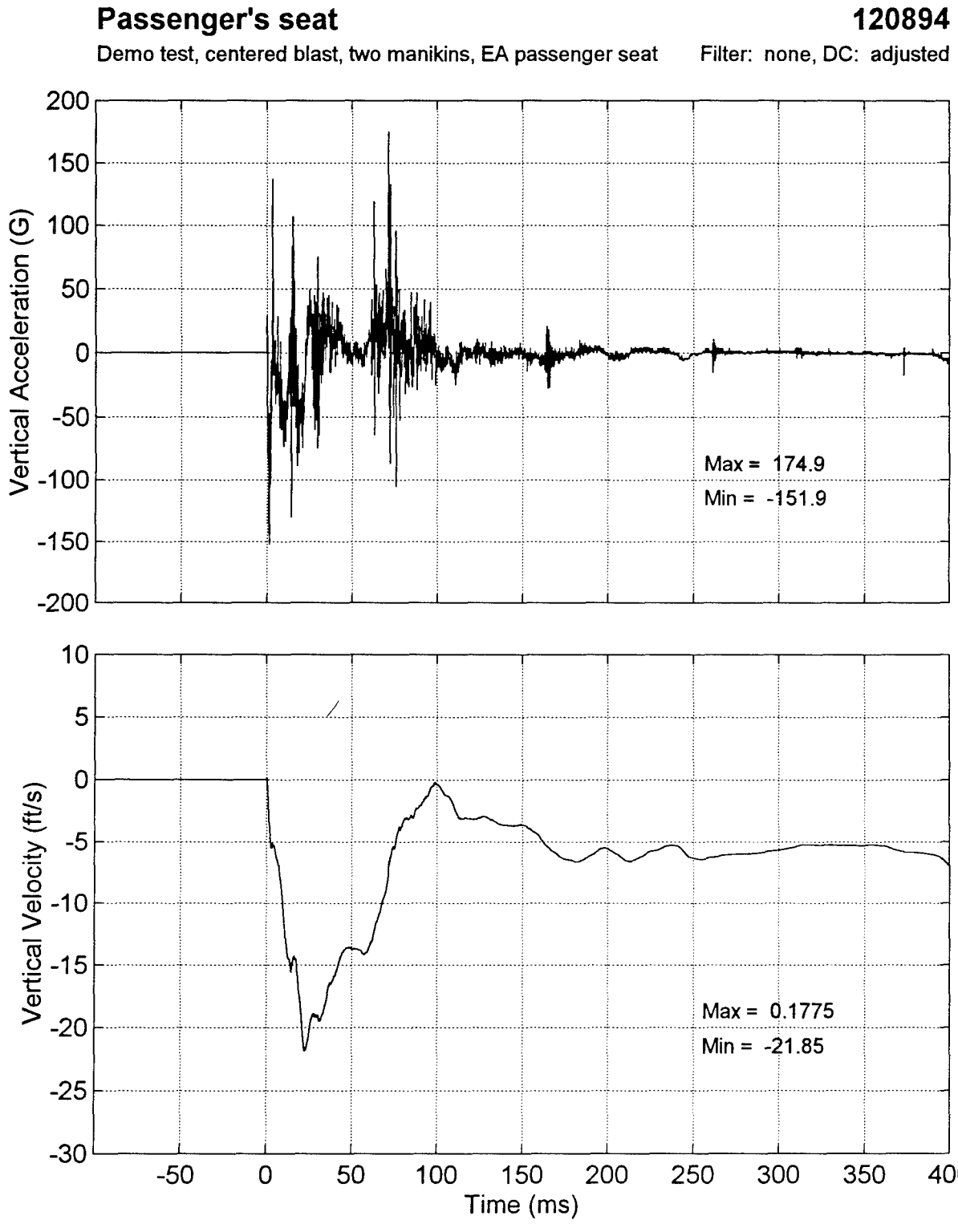

Figure C-4. Acceleration and velocity, assuming that zero level is at end of signal, and after setting pre-trigger segment to zero.

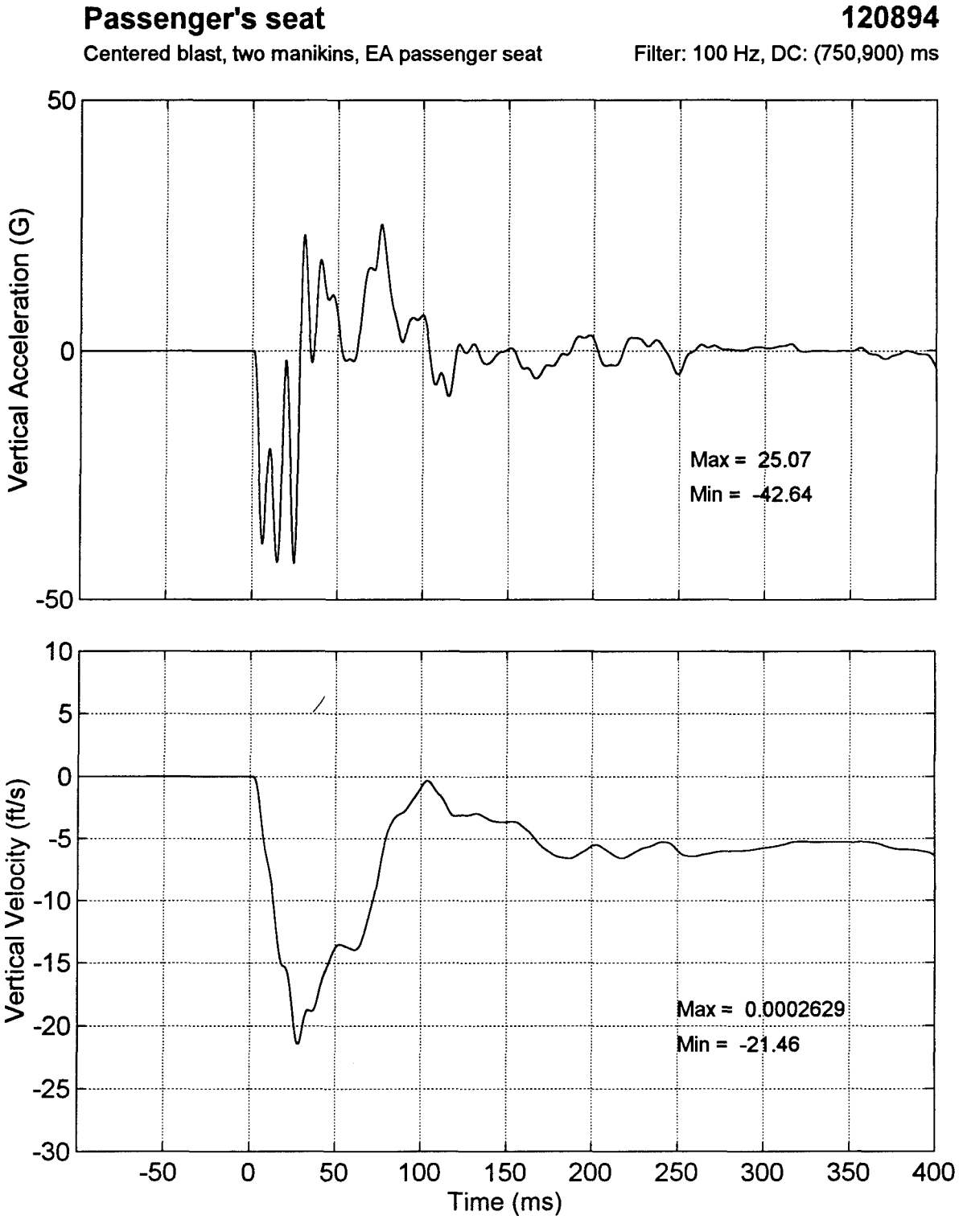

Figure C-5. Filtered acceleration and its integrated velocity, after removal of zero bias.

Appendix D.

Recommended filters and filtering methods

This appendix contains recommendations for filtering impact acceleration and force signals obtained from manikins. Its also includes listing of a pair of computer subroutines, written in Fortran, to design and apply Butterworth filters recursively, i.e., in the time domain.

Table D-1.
SAE J211 recommended filters for impact test instrumentation.

Typical test measurements	Class	Corner
Vehicle accelerations:		
... for gross motion comparison	CFC 60	100 Hz
... for use in simulations	CFC 60	100 Hz
... for integration to velocity	CFC 180	300 Hz
... for integration to displacement	CFC 180	300 Hz
... for component analysis	CFC 600	1000 Hz
Occupant/vehicle interaction:		
Restraint system forces	CFC 60	100 Hz
Belt extension*	CFC 60	100 Hz
Seating system accelerations*	CFC 60	100 Hz
Steering column loads	CFC 600	1000 Hz
Occupant:		
Pelvis accelerations and loads*	CFC 60	100 Hz
Neck loads*	CFC 180	300 Hz
Chest accelerations	CFC 180	300 Hz
Chest deflection	CFC 180	300 Hz
Spinal loads*	CFC 180	300 Hz
Femur force	CFC 600	1000 Hz
Head accelerations	CFC 1000	1650 Hz

* Filters indicated for signals marked with an asterisk are those commonly used by practitioners of crash testing and were not included in early versions of the SAE J211 guideline.

```
""""""""""""""""""""""""""""""""""""""""""""""""""""""""""""""""""""""""""""""""""""""
SUBROUTINE  design_butter (samhz, corner, nsect, acof, bcof)
""""""""""""""""""""""""""""""""""""""""""""""""""""""""""""""""""""""""""""""""""""""
"  Subroutine to design low-pass Butterworth digital filters.  The filter is
"  obtained by using the bilinear transformation to transform analog filter
"  equations to digital domain.  Filtering is accomplished by a cascade of
"  second-order sections which are defined by the order of the filter.
"  Implementation in the time-domain is recursive.  Arguments are:
"
"      samhz  ...  given sampling rate (Hz) of digital signal.
"      corner ...  given filter corner frequency (Hz) where the magnitude
"                        is -3 dB (half-power point).
"      nsect  ...  given number of 2nd-order sections (pole-pairs).  The
"                        number of poles of the filter will be 2 x nsect.
"      acof   ...  coefficients (A0,A1,A2) of 2nd-order filter sections
"      bcof   ...  coefficients (B0,B1,B2) of 2nd-order filter sections
"
"  Recursive filtering through each 2nd-order section is performed by
"  the difference equation:
"
"  Y(n) = A0 * X(n) + A1 * X(n-1) + A2 * X(n-2) - B1 * Y(n-1) - B2 * Y(n-2)
""""""""""""""""""""""""""""""""""""""""""""""""""""""""""""""""""""""""""""""""""""""

REAL*4 acof(3,*), bcof(3,*), pie /3.1415926535/

wc = corner / samhz
fact = TAN( pie * wc )
npoles = 2 * nsect
sector = pie / npoles
wedge =  sector / 2.

DO m = 1, nsect

   ang  = wedge * ( 2*m - 1 )
   xm = - fact * COS( ang )
   ym =   fact * SIN( ang )
   den = ( 1. - xm )**2 + ym**2
   um = ( 1. - xm**2 - ym**2 )/ den
   vm = ( 2. * ym )/ den
   bcof(1,m) = 1.
   bcof(2,m) = -2. * um
   bcof(3,m) = um * um + vm * vm
   sum = bcof(1,m) + bcof(2,m) + bcof(3,m)

   acof(1,m) = sum / 4.
   acof(2,m) = sum / 2.
   acof(3,m) = sum / 4.
END DO

RETURN
END
```

```
"""""""""""""""""""""""""""""""""""""""""""""""""""""""""""""""""""""""""""""""""""""""""""""""
SUBROUTINE  filter_2nd_order (x, npt, a, b)
"""""""""""""""""""""""""""""""""""""""""""""""""""""""""""""""""""""""""""""""""""""""""""""""
"  Subroutine for recursive application of second-order filter to a time
"  domain signal.  Its must be called for each filter section.
"
"  Inside this routine, filtering is forward.  Backward filtering may be
"  accomplished by reversing the signal prior to calling this routine,
"  then restoring the order upon return of the filtered signal.
"
"     x()    ...   upon entry, an array containing the unfiltered signal,
"                        and replaced by the filtered signal upon return.
"
"     npt    ...   number of samples in the x() signal array.
"
"     a()    ...   array containing A0, A1, and A2 coefficients of filter
"     b()    ...   array containing B0, B1, and B2 coefficients of filter
"                  Note:  B0 must be supplied even through not used.
"""""""""""""""""""""""""""""""""""""""""""""""""""""""""""""""""""""""""""""""""""""""""""""""
REAL*4 x(*), a(*), b(*)

a0 = a(1)
a1 = a(2)
a2 = a(3)
b1 = b(2)
b2 = b(3)

xn0 = x(1)
xn1 = 2 * xn0 - x(2)
xn2 = 2 * xn0 - x(3)
yn1 = xn2
yn2 = xn1

yn0  = a0 * xn0 + a1 * xn1 + a2 * xn2 - b1 * yn1 - b2 * yn2
x(1) = yn0

xn2 = xn1
xn1 = xn0
xn0 = x(2)
yn2 = yn1
yn1 = yn0

yn0  = a0 * xn0 + a1 * xn1 + a2 * xn2 - b1 * yn1 - b2 * yn2
x(2) = yn0
yn1 = x(2)
yn2 = x(1)

DO n = 3, npt

   yn = a0 * x(n) + a1 * x(n-1) + a2 * x(n-2) - b1 * yn1 - b2 * yn2

   x(n-2) = yn2
   yn2 = yn1
   yn1 = yn

END DO

RETURN
END
```